BUREAU OF RESEARCH

INNOVATIVE TECHNIQUES AND MATERIALS FOR PREVENTING CONCRETE SHRINKAGE CRACKING
FINAL REPORT

January 2023

Submitted by

Gilson R. Lomboy, D.Eng., Ph.D.
Associate Professor
Rowan University

Douglas B. Cleary, Ph.D.
Professor
Rowan University

Cheng Zhu Ph.D.
Assistant Professor
Rowan University

Shiho Kawashima, Ph.D.
Associate Professor
Columbia University

Palash Badjatya
Graduate Student
Columbia University

Seth Michael Wagner
Graduate Student
Rowan University

NJDOT Research Project Manager
Giri Venkiteela

In cooperation with

New Jersey
Department of Transportation
Bureau of Research
And
U. S. Department of Transportation
Federal Highway Administration

DISCLAIMER STATEMENT

TECHNICAL REPORT DOCUMENTATION PAGE

1. Report No. FHWA-NJ-2023-002	2. Government Accession No.	3. Recipient's Catalog No.
4. Title and Subtitle **FINAL REPORT** Innovative Techniques And Materials For Preventing Concrete Shrinkage Cracking		**5. Report Date** January 2023
		6. Performing Organization Code
7. Author(s) Gilson R. Lomboy, Douglas Cleary, Cheng Zhu, Shiho Kawashima, Seth Michael Wagner, Palash Badjatya		**8. Performing Organization Report No.**
9. Performing Organization Name and Address Rowan University Center for Research and Education in Advanced Transportation Engineering Systems (CREATES) 107 Gilbreth Parkway Mullica Hill, NJ 08062		**10. Work Unit No.**
		11. Contract or Grant No. NJDOT Contract ID Number
12. Sponsoring Agency Name and Address New Jersey Department of Transportation Federal Highway Administration 1035 Parkway Avenue, P.O. Box 600 1200 New Jersey Avenue, SE Trenton, NJ 08625.0600 Washington, DC 20590		**13. Type of Report and Period Covered:** Final Report,
		14. Sponsoring Agency Code FHWA, NJDOT
15. Supplementary Notes		

16. Abstract

Cracks weaken concrete and permit water and harmful chemical ingress into structures. Shrinkage also decreases the load-carrying capacity of bridges. This study investigates shrinkage cracking prevention of infrastructure concretes used in New Jersey. The 15 initial evaluation mixtures were first tested to evaluate their shrinkage behavior. Based on the results of the tests, control mixtures were selected for modification with shrinkage control admixtures and additives. The admixtures and additives were a shrinkage-reducing admixture, a shrinkage-compensating admixture, fibers, an internal curing agent, and two coatings. The modified mixtures were then tested for the effects of the admixtures and additives on shrinkage, mechanical properties, and durability.

The cracking potential of control mixtures ranged from moderate-low to high. Initial evaluation mixture autogenous shrinkage increases with the increasing volume of fine aggregate and decrease of coarse aggregates. On the other hand, increasing the portland cement and total binder while decreasing the amount of fine and coarse aggregates tends to increase the drying shrinkage. Different types of admixtures and additives had varied effects on shrinkage. To mitigate cracking in concrete by using admixtures and additives, the standard restrained ring test ASTM C1581 can be adopted for evaluating the concrete's performance after modification. It is recommended that specifications for concrete shrinkage cracking be met by three specimens from the same batch.

17. Key Words Concrete shrinkage, shrinkage reducing; shrinkage compensating; internal curing; fibers; shrinkage cracking		**18. Distribution Statement** No restrictions.	
19. Security Classif. (of this report) Unclassified	**20. Security Classif. (of this page)** Unclassified	**21. No. of Pages** 56	**22. Price** Leave blank

Form DOT F 1700.7 (8-72)   Reproduction of completed page authorized

ACKNOWLEDGEMENTS

TABLE OF CONTENTS

LIST OF FIGURES

LIST OF TABLES

EXECUTIVE SUMMARY

Cracks weaken concrete and permit water and harmful chemical ingress into structures, thereby accelerating deterioration of concrete and corrosion of reinforcement. Shrinkage also causes concrete slabs to curl and warp, which affects the girder-to-deck composite action, ultimately decreasing the load-carrying capacity of bridges. This study investigates shrinkage cracking prevention of infrastructure concretes used in New Jersey.

Fifteen mixtures were first evaluated on their shrinkage behavior. The shrinkage tests used were autogenous shrinkage, drying shrinkage, and restrained ring shrinkage cracking. Based on the results of the tests, control mixtures with high shrinkage potential were selected for modification with shrinkage control admixtures and additives. The admixtures and additives were a shrinkage-reducing admixture (SRA), a shrinkage compensating admixture (SCA), an internal curing agent, which was a fine lightweight aggregate (LWA), fibers, and two surface coatings. The surface coatings were lithium silicate (LS) and a polymer-modified cementitious binder (EN). The surface coatings were designed for surface strengthening but were included to investigate if they affected concrete shrinkage.

The modified mixtures were then tested for the effects of the admixtures and additives on autogenous shrinkage, drying shrinkage, and restrained shrinkage. The mechanical properties of the modified mixtures were also measured. These mechanical properties were compressive and tensile strength, elastic modulus, and creep. The modified mixtures were also tested for electrical resistivity and resistance to cyclic freezing and thawing to evaluate their durability. Finally, small slabs made from the modified mixtures were exposed to field conditions to measure their shrinkage behavior.

The results showed that the cracking potential of the original fifteen mixtures ranged from moderate-low to high. The mixture autogenous shrinkage increases with the increase of fine aggregate volume or decrease of coarse aggregate volume. On the other hand, an increase in portland cement and total binder while decreasing the amount of fine and coarse aggregates tends to increase the drying shrinkage. Incorporating admixtures and additives in the two selected control mixes had varying effects on autogenous, drying, and restrained ring shrinkage. The SRA was effective at reducing the concrete's shrinkage and cracking potential. The SCA did not reduce the autogenous shrinkage of the concrete but reduced the drying shrinkage when the maximum dosage was used. Surface coating EN slightly reduced autogenous and drying shrinkage. However, LS reduced autogenous shrinkage but not the drying shrinkage. Internal cuirng with LWA reduced the autogenous shrinkage and cracking potential but not the drying shrinkage. Also, incorporating fibers reduced the autogenous shrinkage and the cracking potential. The SRA, SCA, fibers, LS, and EN do not adversely affect concrete's strength and elastic modulus. It was also observed that SRA was more robust than SCA in reducing shrinkage when exposed to field conditions.

1

To mitigate cracking in concrete by using admixtures and additives, the standard restrained ring test ASTM C1581 can be adopted for evaluating the concrete's performance after modification. However, it was observed that the cracking age in a restrained ring test could greatly vary, even for specimens from the same batch. Therefore, specifications for concrete shrinkage cracking should be met based on three specimens from the same batch to be approved. This reduces the risk of failures due to incompatibility, processing, and testing.

INTRODUCTION

Background

Modern concretes used in transportation infrastructure have high and rapid strength development, lower permeability, and excellent durability. However, because of the high cementitious content, low water-to-cementitious material ratio (w/cm), and various admixtures, modern concrete in transportation infrastructure often possess a high risk of shrinkage cracking. Over the past decade, many states have reported cracking on transportation infrastructure, particularly on bridge decks at early ages (1, 2), which is also a concern in New Jersey.

Cracks weaken concrete and permit water and harmful chemical ingress into structures, thereby accelerating deterioration and corrosion of reinforcement (3). Shrinkage also causes concrete slabs to curl and warp, which affects the girder-to-deck composite action, ultimately decreasing the load-carrying capacity of bridges (4). In addition, shrinkage may bring about stress loss in prestressed concrete structures and affect the camber and deflection of bridge girders.

To assess the cracking risk of infrastructure concrete, it is essential to understand the shrinkage behavior (such as shrinkage components, amount, and progression time) of concrete. And to control cracking, it is necessary to compensate for the effects of material constituents (i.e., cementitious materials, aggregate, and admixtures) on concrete shrinkage behavior (5, 6, 7).

This study investigates shrinkage cracking prevention of infrastructure concretes used in New Jersey. More specifically, it is to identify the significant shrinkage components (autogenous and drying shrinkages) currently present in New Jersey concretes known to have had issues with shrinkage and the application of recent innovations (shrinkage reductions, compensation, internal curing, coatings, and fibers) in shrinkage cracking mitigation. In addition, the research quantifies the magnitude of the shrinkage processes operating in NJDOT approved concrete and how cracking prevention measures impact these shrinkages.

Objectives

Modern concrete mixtures used in transportation infrastructure can have a high risk of shrinkage cracking because of the high cementitious content, finer portland cement, low water-to-cementitious material ratio (w/cm), and the various admixtures in the concrete. The study aims to improve the longevity and performance of New Jersey transportation infrastructure by reducing the concrete shrinkage and cracking potential and limiting the ingress of water and other deleterious substances into the concrete. Innovative techniques and materials for preventing shrinkage were studied in New Jersey materials and conditions to achieve this goal. The following set of specific objectives was set:

1. To identify and measure components of shrinkages in New Jersey concretes;
2. To identify and investigate different methods for controlling shrinkage cracking applicable to New Jersey infrastructure concrete mixes.
3. To determine the effects of the techniques and methods used to control shrinkage cracking on other fresh and hardened concrete properties.

4. To investigate the field performance of the New Jersey mixes and compare concrete mixes with different shrinkage cracking potentials and concrete mixes with and without shrinkage control methods.

Approach

The research first reviews the literature on techniques and materials for reducing concrete's shrinkage and cracking potential. Next, shrinkage tests were conducted on selected NJDOT-approved concrete mixtures. The results of the tests were used in identifying control mixtures to be treated for reducing shrinkage and cracking potential. Then, shrinkage-reducing admixture, shrinkage-compensating admixture, internal curing, coating, and fibers were added to the control mixtures. The treated mixtures were tested for changes in shrinkage behavior and cracking potential in comparison to the controls. Furthermore, the shrinkage cracking mitigation effectiveness, effects on fresh, short and long-term hardened properties, durability, and performance in New Jersey field conditions were investigated.

The following sections of the report provide a summary of the literature review. Then, the materials and mixtures studied are given. This is then followed by the test methods implemented for measuring concrete properties. Finally, conclusions and recommendations based on the study are provided.

LITERATURE REVIEW

Shrinkage Behavior and Shrinkage Induced Cracking of Concrete

Concrete shrinkage generally occurs from plastic shrinkage, chemical shrinkage, autogenous shrinkage, drying shrinkage, carbonation shrinkage, and their combinations. In these cases, the paste in concrete is what changes in volume. The factors that significantly affect concrete shrinkage are types of cementitious materials, w/cm, water or paste content, aggregate type, fine-to-coarse aggregate ratio, environmental conditions, and structure configuration.

Chemical and Autogenous Shrinkage

Chemical shrinkage results from the lesser volume of the cement hydration products compared to the unreacted constituents. The reduction in volume is related to the chemistry and degree of hydration of cementitious materials.

Autogenous shrinkage is a measurable external volume change occurring when concrete has no moisture transfer to the surrounding environment. It occurs during the plastic state and continues during the hardened state. In its plastic state, shrinkage occurs due to the change in the volume of the paste. In the hardened state, continuing hydration consumes the water in concrete and thereby developing water menisci in the fine pores. The water menisci generate stress in the pore walls that causes the concrete to shrink. As concrete reaches a hardened stage, self-desiccation results in shrinkage. Different from chemical shrinkage, autogenous shrinkage is an external volume reduction.

Yun and Jan (8) studied concrete shrinkage focused on field conditions and their effect

4

on the material. The experimental procedure was designed to simulate actual field conditions in terms of uncontrollable variables such as temperature and humidity. To replicate the real environment, the concrete castings were immediately covered to prevent water contamination. Conclusions that were drawn from this experiment were that the maximum amount of autogenous shrinkage occurs within 24 hours; timely water curing can reduce the shrinkage of high-performance concrete; reinforcing bars, although barred from HPC, would decrease the amount of shrinkage; and lastly, that lower water-to-cement ratios also lead to higher autogenous shrinkage.

Lee et al. (9) found that at the same w/cm ratio, ground granulated blast furnace slag (GGBFS) concrete exhibited higher autogenous shrinkage than the control concrete. They suggested that GGBFS replacement level and particle shape greatly contributed to the high level of shrinkage. Persson (10) studied the use of silica fume and observed that autogenous shrinkage mainly results from the pore refinement and decline of the internal humidity in concrete. Whitling et al. (2) focused on the trends in cracking and drying shrinkage of silica fume concretes for highway bridge decks. They found that silica fume did not affect early-age concrete cracking unless the concrete was improperly cured. However, silica fume concretes exhibit more shrinkage in the early stages than their traditional counterpart and thus require a 7-day continuous moist conditions plan for proper curing.

Yang et al. (11) sought to separate the autogenous shrinkage strain from the drying shrinkage strain of high-strength concrete with silica fume at early ages. The bound water content (BWC) method was used, whereby samples of varying water/cement ratios were left in sealed conditions to establish a relationship between hydration and autogenous shrinkage. This allowed for the distinguishing between autogenous and drying shrinkage when examining samples left in unsealed drying conditions. It was found that autogenous shrinkage accounted for 20-50% of the total shrinkage using the BWC method, and drying shrinkage became dominant as the water/cement ratio increased.

Plastic Shrinkage and Drying Shrinkage
Plastic shrinkage occurs in fresh concrete when the rate of water evaporation on a concrete surface is higher than the rate of water bleeding inside the concrete. An effective way to control plastic shrinkage is to control the rate of water evaporation on the concrete surface. Micro-cellulose fibers have also been effectively used to reduce plastic shrinkage cracking. One critical step to ensure proper function was to disperse the fibers to maintain consistency. When dispersion was adequately performed, the fibers possessed internal curing capabilities but not enough for exclusive application. In addition, the fibers proved to be efficient in significantly reducing the drying shrinkage-induced cracking. Kawashima and Shah (12) analyzed the behavior of cementitious materials that have cellulose fibers under sealed and unsealed conditions. Sealed conditions simulate autogenous shrinkage, and the unsealed condition mimics dry shrinking. Some key conclusions were that the fibers controlled drying shrinkage, the cellulose fibers also provided some internal curing, and the improved distribution of the fibers resulted in more desirable properties.

Drying shrinkage results from water loss in hardened concrete. When concrete is

exposed to drying conditions, concrete shrinks when the water leaves due to the rise of capillary tension, surface tension, and disjoining pressure.(13) When the ambient relative humidity (RH) is sufficiently low, the interlayer water in C-S-H gel in concrete may also be removed and cause the concrete to shrink. Drying shrinkage is closely related to the amount of water, the structure (size and distribution) of the pores, and the chemistry of the pore solutions in concrete. In the study by Rougelot(13), autogenous shrinkage was controlled by desaturation. This was done by saturating samples for 5 months in a lime-saturated bath. Beams were then left in a controlled environment, and humidity was lowered from 100% to 12% over the following months. It was determined that slopes of the shrinkage curves decrease with decreasing humidity and that higher water-to-cement ratios lead to increases in desiccation shrinkage and porosity.

Carbonation Shrinkage

Carbonation shrinkage occurs when cement constituents and cement hydration products in concrete react with carbon dioxide (CO_2) in the air. When the concrete reacts with the carbon dioxide, the weight of the concrete increases, and an irreversible reaction resulting in carbonation shrinkage occurs. The carbonation process proceeds slowly and usually produces slight shrinkage at a relative humidity below 25% or near saturation.

Carbonation sometimes occurs in cold weather regions that implement gas heaters to aid in curing. One of the gases produced by the heaters is carbon monoxide which, when in contact with concrete, produces a light and chalky finish on the surface of the concrete.

Shrinkage Induced Cracking

Restrained autogenous shrinkage in high-strength concrete can produce stresses during the early ages that may cause premature cracking. This was shown by Igarashi et al. (14), mainly when the ratio between the restraining stress and the tensile strength approached 50%. By comparing restrained and unrestrained samples of varying water-to-cement ratios and silica fume contents, it was found that restraint of autogenous shrinkage in high-strength concrete at early ages caused high internal stress and large creep strain. This caused internal stress to be lower than expected. Lower water-to-cement ratios and higher silica fume content increased the creep strain in restrained autogenous shrinkage tests at early ages, which in turn increasingly lowered the magnitude of the internal stress. It was also found that when the ratio of restraint-induced internal stress to tensile strength approached 50%, premature cracking began to occur, leading to tensile failure. Darquennes et al. (15) found that the shrinkage cracking occurred later than the portland cement concrete in the case of slag cement concrete. Despite a larger autogenous shrinkage, it took longer for the slag cement concrete to crack than the portland cement concrete due to the expansion of the cement matrix in the slag concrete at an early age and the large capacity to relax internal stresses.

The effect of reinforcement on early-age cracking in high-strength concrete was investigated by Sule and van Breugel (16). The effects of reinforcement on early-age cracking in high-strength concrete due to autogenous shrinkage and thermal effects

were studied. A temperature stress testing machine was used to restrain the sample and to control curing temperatures. High-strength concrete was compared with normal strength, while the reinforcement percentages and number of reinforcement bars were varied. The samples were tested isothermally and semi-adiabatically to distinguish between autogenous shrinkage and thermal effects. It was found that the formation of smaller cracks delays the appearance of major cracks. Cracking was comparable in the plain and single-bar concrete but was more delayed in the four-bar concrete due to its higher tensile strain capacity. The reinforcement percentages studied were 0, 0.75, 1.34, and 3.02% and were configured with one and four reinforcement bars. The researchers showed that reinforcement quantity and distribution could induce the formation of smaller cracks. These smaller cracks can postpone the moment at which major cracks are formed.

Concrete Shrinkage and Control Technologies

There are various ways to control concrete shrinkage and shrinkage cracking. For example, in addition to the commonly used concrete jointing (e.g., saw cutting), Mindess and Young (17) suggested altering concrete shrinkage behavior through mix design optimization, such as reducing water content and increasing aggregate/concrete stiffness. In addition, Leepage et al. (18) demonstrated that improved curing practices could help reduce concrete shrinkage. Recently, as high-performance concrete, which often has high shrinkage cracking potential, is increasingly used in transportation infrastructures, breakthroughs have also been made for concrete shrinkage control, including using shrinkage-reducing admixtures (SRAs), shrinkage compensating admixtures (SCAs) and internal curing (IC) agents.

Shrinkage Reducing Admixtures (SRAs)

SRA is a chemical admixture that reduces fluid surface tension in concrete pores (19, 20). The surface tension is the driving force of concrete drying shrinkage. SRA can delay the cracking age and reduce the corresponding crack width (21, 22).

Zhan and He (23) published a review of the application of shrinkage-reducing admixtures in concrete. The review covered characteristics of SRA, hydration, workability, mechanical properties, durability, and dimensional stability. Zhan and He drew the following conclusions based on their review of prior studies.

- SRA delays the hydration reaction of concrete at early ages and improves the hydration at later stages. Hydration is sensitive to curing conditions. There is no clear effect on the workability of concrete.
- A majority of studies indicate strength properties of SRA concretes are reduced as SRA contents are increased. Using fibers and moisture curing can improve the properties of SRA concretes.
- SRA generally decreases water absorption and chloride permeability and increases resistance to freeze-thaw.
- SRA can reduce autogenous shrinkage, drying, plastic, and chemical shrinkage. The shrinkage reduction mechanism of SRA on the various types of shrinkage is similar. It is mainly due to the reduced surface tension,

reduced concentration of pore solution ions, adjusted relative humidity, and expansion effect.
- The combined use of SRA and other components or admixtures, such as expansive agents and internal curing agents, has a better effect on reducing shrinkage.
- SRA reduces the creep of concrete.

Wang et al. (24) studied the effect of shrinkage-reducing admixture on high-performance concrete with Type I cement, coarse limestone aggregates, river sand, water reducer, and air-entraining admixture. The results show that SRA effectively reduces shrinkage strains and strain rates with increasing dosage. The dosages used were 0, 0.5, 1, and 1.5 times the manufacturer's recommended dosage.

Wei et al. (25) studied the effect of SRA-modified nanosilica (NS@SRA) on the autogenous shrinkage of cement paste using the restrained ring test. NS-added paste exhibits much higher residual tensile stress than plain paste from the beginning of the test to its cracking time. In contrast, paste with NS@SRA shows a higher rate of stress development than plain paste only at the measurement's beginning. Furthermore, cement paste's time-to-cracking (defined as the difference between the age when a sudden decrease in tensile stress occurs and the age of initial drying) is reduced by 11.7 h with NS addition. In contrast, incorporating NS@SRA particles extends the time-to-cracking of cement paste by 11.6 h. These results demonstrate NS@SRA's capability to alleviate shrinkage and cracking risks of cement paste with low w/c.

Shrinkage Compensating Admixtures (SCAs)

SCA is a chemical admixture that offsets concrete shrinkage through expansion from chemical reactions during an early age. The common types of SCA are Type K cement, Type G additive/component, and MgO-based additive. Type K cement attributes its expansion from ettringite formation from a sulfoaluminate-based agent. Type G additive forms calcium hydroxide platelet from a lime (CaO)-based expansive agent. MgO (periclase) additive hydrates to form $Mg(OH)_2$ (brucite) (26, 27, 28). A sulfoaluminate-based SCA commonly has a slower expansion rate than a lime-based SCA, the latter more suitable for early-age strength concrete with a short curing time (29). SCAs are also used to produce expansive types of cement (such as Types K, M, and S cement) (ASTM C845). Wang et al. (30) studied the effect of MgO-based SCA on high-performance concrete. The results showed a limiting dosage for free drying shrinkage reduction. However, the SCA is still effective in reducing shrinkage strains under restrained conditions.

Wei has studied the drying shrinkage and associated restrained cracking behaviors of cementitious composites embedded with stiff (quartz) and soft (phase change material, PCM) inclusions (25, 31). The results show that increasing the quartz volume fraction reduces the drying shrinkage of the composite since stiff inclusions restrain the shrinkage of the paste. While PCM inclusions do not significantly alter the drying shrinkage of cement paste, the addition of PCMs enhances the cracking resistance of cement-based materials. Besides PCMs' hydrophilic nature, composites containing soft inclusions demonstrate benefits from crack blunting and deflection and improved stress

relaxation. Consequently, although the residual tensile stress at failure in the restrained ring test remains similar, the time to failure (i.e., macroscopic cracking) of PCM-containing composites is considerably extended.

Mo et al. (32) studied the influence of calcination conditions on the expansive properties of MgO-type expansive agents (MEA) used in cement-based materials. A single MEA particle consists of many aggregated MgO grains. The specific surface area and the activity of the MgO grain structure influence the hydration activity of MEA. Higher calcination temperature and longer residence time cause grain growth of MgO. This produces a decrease in inner pore volume and specific surface area and decreases the hydration activity of MEA. The self-expansion of MEA particles due to the hydration of MgO grains causes the expansion of cement paste. Highly active MEA hydrates rapidly and produces fast early-age expansion. A short time is needed to reach the maximum expansion. MEA with lower activity hydrates slowly, resulting in less early-age expansion. After an induction period, the sintered MgO grains are broken down by the expansion at the grain boundary. This increases the reaction area and accelerates the hydration and the corresponding expansion. Less active MEA has a longer induction period, producing a larger final expansion. Mo et al. suggest that the expansion properties of MEA could be regulated by controlling its microstructures and hydration activity by changing the calcining temperature and residence time to produce MEA with various expansion properties.

Expansive admixtures based on calcium sulphoaluminate (CSA) produce expansive ettringite. CSA produces expansion at later ages than that induced by CaO. This expansion, therefore, occurs after the compressive strength starts to grow. Because of the later start to the expansive reactions, CSA-based expansive admixtures require a longer wet cure. Monosi et al. (33) reported on the effectiveness of an expansive CSA-based admixture with propylene-glycol ether-based shrinkage-reducing admixture. Monosi et al. report

- The mortar-free expansion increases with the gypsum content, and the water/binder used.
- There is a threshold water/binder value below which only shrinkage occurs.
- The SRA admixture strongly amplifies the free mortar expansion. However, it does not amplify the amount of free contraction nor the time to reach the steady state.
- In the presence of restraint, the SRA admixture does not affect the mortar expansion but slightly reduces the restrained shrinkage.
- The SRA slightly delays ettringite formation but significantly changes the ettringite fibers' morphology, resulting in a finer structure.
- SRA reduces the compressive strength of mortars, particularly at early ages.

Based on these findings, it was concluded that SRA, combined with CSA expansive admixtures, does not improve performance much in the restrained scenario. Still, it could be a helpful addition to CSA-based shrinkage-compensating cementitious materials where reinforcements are absent.

In another study using a calcium sulphoaluminate (CSA) based expansive agent, Dong

et al. (34) considered the shrinkage of self-compacting concrete using a comparator. They performed qualitative and quantitative analyses of the hydration products using X-ray diffraction. In the concrete mixes, the total cementitious content was held constant while varying the replacement of portland cement with 0 percent to 40 percent fly ash and slag at a ratio of 3:2. The amount of CSA-based expansive agent was held constant at approximately 11 percent of the cement content. Samples were cured in water, wet three times per day, or in ambient room conditions. When specimens were cured in water, as the amount of mineral admixture was increased, the expansion of the specimens also increased with the greatest expansion with 40 mineral admixture replacement of portland cement. Under the intermittent wetting and ambient curing conditions, combining mineral admixtures and shrinkage compensating agents reduced the shrinkage by about 16 percent in the former case and 13 percent in the latter. With intermittent curing, shrinkage was held under 250 microstrains, while it was over 600 microstrains in the ambient condition.

Zhu et al. (35) presented the shrinkage behavior of calcium hydroxide-added alkali-activated slag concrete (AAS). AAS concrete is an alternative to portland cement concrete. It has properties that include rapid compressive strength development and high sulfate resistance. It also has high shrinkage. It was found that the addition of $Ca(OH)_2$ increased the plastic shrinkage of AAS concrete but reduced autogenous and drying shrinkage through changes in the reaction rates and the hydration products.

- The addition of $Ca(OH)_2$ into AAS concrete enhanced the development of compressive strength and the static elastic modulus at an early age, especially when the W/B ratio is high. However, the degree of hydration was not increased in the long term but significantly increased at an early age.
- The fast hydration due to the addition of $Ca(OH)_2$ significantly increased the plastic shrinkage with a decrease of the mass loss in 24 h.
- Autogenous and drying shrinkage mass loss of AAS concrete was reduced by adding $Ca(OH)_2$. The increasing Ca/Si ratio of C-S-H(I) gel and crystals in AAS concrete are responsible for decreasing the autogenous and drying shrinkage.

Ye and Radlinska (36, 37) investigated the shrinkage mechanisms in AAS concrete and mitigation strategies. Compared to ordinary portland cement concrete, AAS shows considerably high drying shrinkage and moisture loss, regardless of exposed relative humidity. A pronounced viscous characteristic in AAS strongly depends on the experienced relative humidity during curing. The viscous performance in AAS is due to the rearrangement and reorganization of C-A-S-H particles (layered sheets) under the capillary stress. The reorganized structure is difficult to modify, meaning most of the shrinkage in AAS dried at high RH is irreversible. Mitigation strategies investigated were high-temperature curing, sulfate enrichment, and calcium enrichment. High-temperature curing reduced the shrinkage of AAS by improving the coalescence or bonding between adjacent C-A-S-H nanoparticles. However, mitigating shrinkage through early-age expansive reactions is less effective since the dominant component of drying shrinkage in AAS is due to the long-term visco-elastic/visco-plastic deformation of C-A-S-H.

Jia et al. (38) studied the effects of calcium sulphoaluminate type expansion agents

(CSAE), CaO type expansion agents (CE), and shrinkage-reducing agents (SRA) on AAS mortars. The addition of CSAE, CE, and SRA decreased the drying shrinkage of AAS mortar by about 41–45%, 54–56%, and 35–44% at 56 d, respectively. However, the internal relative humidity conditions in the various AAS mortars within 56 d did not evolve similarly. The consumption of a large amount of water during the formation of AFt, meant the addition of CSAE caused a significant decline of internal relative humidity in AAS mortar in the first three days. The internal relative humidity at the early ages remained stable for the CE and SRA group mortars. At late ages, the internal relative humidity in the three groups with admixtures became higher than in the reference group. The formation of crystal phases, AFt and CH, contributed to the decline of the drying shrinkage of AAS mortars. However, CE is more effective in reducing drying shrinkage than CSAE. This was attributed to the comprehensive effect of both low water consumption of CaO during the hydration process and the high elastic modulus of CH in the CE group.

Haiyan et al. (39) studied the freeze-thaw durability of high-strength concrete, high-strength concrete with an added expansive agent, and high-strength concrete with an expansive agent and steel fibers. The concrete studied was not air-entrained. Binders included portland cement plus a blend of 10 percent silica fume, 20 percent fly ash, and 20 percent slag by mass of cementitious materials. An aluminate expansive agent was used. The freeze-thaw life of the high-strength concrete with the expansive agent was shorter than that of the high-strength concrete by 34 percent. The cause was explained by the greater production of calcium aluminate monosulfate in the concrete with the expansion agent. This converts to calcium aluminate trisulfate during the freeze-thaw cycles, and the resulting volume expansion increases the internal pressure. The addition of steel fibers can restrain the spread of internal cracks.

Internal Curing (IC) Agents

Internal curing is a mitigation strategy for autogenous shrinkage where additional curing water is provided to the hydrating cement matrix through the inclusion of water-saturated porous materials (SLA) (40) or saturated super absorbent polymer particles (SAP) (41, 42) in a concrete mixture. The key advantage of internal curing over conventional external curing methods is that it can significantly reduce the distance that additional curing water must travel to access the hydrating paste and replenish its emptying capillary pores. The supplied water from these saturated particles balances the moisture lost in concrete caused by drying or self-desiccation, thus reducing shrinkage and cracking. SAP can absorb up to 5000 times its weight. Another benefit of internal curing is increased compressive strength at later ages due to increased hydration (43). Although such a curing method is typically not necessary for normal-strength concrete, it becomes increasingly critical for high-strength or high-performance concretes with low water-to-cement ratios and/or incorporating reactive mineral fillers, e.g., silica fume, thereby exhibiting denser capillary pore structure and self-desiccation.

Various forms of porous inclusions, commonly referred to as internal curing (IC) agents, have been investigated to employ internal curing. Among the IC agents, the most common are lightweight aggregates (44, 45, 46, 47, 48, 49, 50) and superabsorbent polymers (51, 41, 42). Other candidate materials that have been investigated include

ceramic waste aggregates (52), rice husk ash (53), coal bottom ash (54), recycled aggregate concrete (55), and wood-derived materials (56).

Lightweight aggregates (LWA) can be incorporated into concrete by replacing normal aggregates, where the replacement level depends on the mix design. Bentz et al. (57) proposed mix proportioning with saturated LWA to prevent self-desiccation based on Powers's mod. It has been demonstrated that autogenous shrinkage can be eliminated at the appropriate dosing. There are various natural and artificial porous aggregates, such as pumice, expanded shale, and expanded clay. Ghourchian et al. (58) have investigated other types, such as zeolite aggregate. However, these were unsuccessful due to their fine pore structure, which hindered water release. The main shortcoming of utilizing LWA is that strength reduction is commonly observed due to its porous nature. However, Zhutovsky et al. (50) suggest that an optimal dosage of saturated LWA can provide enough internal curing water to sustain hydration while overcoming any strength reduction accompanying the porous inclusions in the matrix. Golias et al. (59) investigated the influence of the initial moisture content of the LWA for internal curing (oven-dried, 24h pre-wetted, vacuum saturated). It was found that oven-dried LWA could absorb mixing water before setting and effectively release as internal curing water later. This demonstrated the potential of introducing LWA dry (versus pre-saturated) as long as the mix is appropriately designed to include additional curing water.

In addition to mitigating autogenous shrinkage, Espinoza-Hijazin and Lopez (60) found that saturated LWA can help to increase the degree of hydration and improve transport properties of higher w/c ratio concretes. Villarreal et al. (61) found beneficial effects of saturated LWA in field applications in concrete paving, for example, reduction or elimination of plastic shrinkage, drying shrinkage cracking, and self-desiccation, as well as improved hydration and increased compressive strength. De la Varga et al. (62) studied high-volume fly ash concretes with low water-to-binder ratios to offset slow hydration and delayed setting. The incorporation of saturated LWA improved early-age strength gain and reduced shrinkage at later ages through internal curing. Cusson et al. (63) conducted a service life and life-cycle cost case study on high-performance concrete (HPC) bridge decks. They found that HPC with SCM and internal curing via LWA exhibited more than 20 years of service life compared to HPC. Cost reductions were 63% compared to normal concrete, despite higher initial costs of HPC and saturated LWA, primarily due to reduced shrinkage and associated reduction in chloride penetration.

Superabsorbent polymers (SAP), also known as hydrogels, are considered the more "straightforward" approach to internal curing than saturated LWA. SAP are polymeric materials that absorb and retain a large amount of liquid without dissolving. SAP may be added as a dry admixture as it can rapidly absorb water during the mixing process. The size of the SAP may be controlled, allowing control of the pore size distribution in the cement paste matrix (41). The main drawbacks of SAP are that they are more costly than LWA, and they can be crushed during the mixing process, which causes them to release water prematurely. Craeye et al. (64) investigated the use of SAP in HPC bridge decks. They found that they can help reduce autogenous shrinkage and associated early-age cracking but reduce mechanical strength, modulus of elasticity, and higher creep deformation. Justs et al. (65) studied the use of SAP in ultrahigh-

performance concrete (UHPC) with water to cement ratio of 0.25. SAPs increased the degree of hydration and mitigated autogenous shrinkage. Although they decreased mechanical strength compared to the control, 150 MPa 28-day strength was still achievable.

Justs et al. (65) studied SAP for internal curing in cement pastes and ultra-high-performance concrete with water to cement ratio below 0.25. Using SAP particles less than 0.63 μm in a mix with a water-to-cement ratio of 0.15 plus an additional 0.05 entrained water to cement in the SAP (total w/c = 0.20) reduced autogenous shrinkage from more than 600 μm/m to about 120 μm/m at 30 days. The same effect was not seen in a comparison mix with a water-to-cement ratio of 0.20 but without SAP. Using a smaller amount of SAP did not produce the same effect.

Although internal curing is an effective mitigation strategy for self-desiccation and subsequent autogenous shrinkage, there are discussions over which features of the IC agents are the most critical to consider. IC features are particle size, pore structure, water absorption, and water release rate. Bentz et al. (66) extended an existing hydration model to incorporate internal curing with LWA. The results suggested that the dispersion of LWA with a finer grain size leads to better efficiency due to the aggregate-paste proximity. The adequate dispersion allows the hydrating paste closer access to the additional curing water. On the other hand, Zhutovsky (50) found the opposite with experimental results that showed coarser LWA is more effective in reducing autogenous shrinkage than finer LWA. This was attributed to the larger pore structure of the coarser LWA allowing the water to escape more readily.

A round-robin study by Mechtcherine et al. (67) showed that key parameters for determining the effect of SAP on shrinkage mitigation, mechanical properties, and workability include shape and size of the SAP particles, as well as absorption and desorption behavior (i.e., release rate) in cement pore solution. The release rate is highly dependent on the chemical composition of the SAP, which affects swelling kinetics and gel network size (68). Studies also suggest that the best suitable IC agent should be determined on a case-by-case basis, depending on the cement paste properties. Zhutovsky et al. (50) studied the efficiency of saturated LWA in concrete with silica fume. Results showed that the efficiency of coarser LWA dropped dramatically between silica fume concrete with a w/c = 0.25 – 0.33, while there was no significant decline with the finer LWA. This study implied that in pastes with mineral admixtures (e.g., silica fume), well-distributed, finer IC agents would be more suitable because the more disconnected pore structure limits the "sphere of influence" through which water can travel.

Coatings/Concrete Densifiers

Baltazar et al. (69) describe surface treatments used to extend the life of new or existing concrete. These surface treatments are classified into three groups. First, hydrophobic impregnations produce a water-repellent surface with no pore filling. Second, impregnations reduce surface porosity by totally or partially filling concrete pores. Finally, coatings produce a continuous protective layer along the concrete surface. Some of these surface treatments can penetrate the concrete pores and react with the hydration products of concrete, reducing the surface porosity and increasing

the superficial strength.

Concrete coatings or concrete densifiers help limit fluid movement out of the concrete, resulting in shrinkage. The most common pore-blocking coatings are silicate-based, such as sodium silicates, potassium silicates, lithium silicates, or a combination. A newer technology is a colloidal silica densifier. Silicate coatings penetrate and react with calcium hydroxide to form calcium silicate hydrate (CSH), the hydration product of cement that contributes the most to strength and density. The studies described below looked at surface hardeners' contribution to fluid transport in concrete.

Muhammad et al. (70) provide a review of implemented approaches to waterproofing concrete through a review of over 100 studies on the topic. The agents are classified by material structure (macro, micro, or nano), by method of application (surface coating or mixture incorporated), and by function (thin coating forming, concrete pore lining additives, or pore blocking additives). The macro materials used are silanes and siloxanes, which could reduce water absorption by 89 percent and 75 percent, respectively. The silane or siloxane-based materials create a water-repellent pore surface while leaving the pores open. Silicates containing compounds such as ethyl silicate, sodium silicates, and other silicates were another macro material used and reduced water absorption by 98.5 percent. Silicate-based materials are pore blockers that change the pore structure and densify the concrete. Micromaterials were polymers and their dispersions and emulsions. While effective in reducing water absorption and chloride ingress, long-term durability issues were identified. Nanomaterials were nan-SiO_2, ZnO_2, and nano clay incorporated to improve water repellency. Thin coating surface forming additives reduced water absorption and penetration depth by 98.96 percent and 94 percent, respectively. Concrete pore lining forming additives reduced chloride and water ingress by 86 percent and 98 percent, respectively. Pore blocking additive reduced water and chloride absorption to 98.5 percent and 48.3 percent, respectively.

Pan et al. (71) also reviewed the performance of concrete surface treatments. Based on their evaluation of the available literature, they report:

- Silica-based treatment can prevent the loss of concrete compressive strength after exposure to elevated temperatures.
- Most surface treatments can reduce the water permeability of concrete.
- In most cases, surface treatments can prevent the ingress of aggressive substances. Polymer coatings are more efficient than other treatment methods in chloride resistance.
- For carbonation retardation, polymer coatings showed better effects than other treatment methods. Silicate-based treatments provide better protection than silane and siloxane, which hardly prevent the ingress of CO_2.

Moon et al. (72) evaluated three levels of concrete protection using inorganic coatings. The first level of protection was a spray-applied prime coating with active components of sodium silicate, potassium silicate, and colloidal silica. The second level of protection was a spray-applied layer of a material with calcium silicate as the main component over the initially primed layer. The highest level of protection was the spray-applied acrylic-silicon layer over the previous two layers. The concrete's protection was then

evaluated through carbonation, chloride penetration, and freeze-thaw tests. Chloride permeability was greatly reduced with each subsequent level of protection for both low and high-strength mortars, with the largest reduction from the addition of the second level of protection. This was explained by the hydration of calcium-silicate, the main component of the inorganic coating. The calcium-silicate generates an insoluble silicate compound after its reaction with the components present at the surface of the mortar. This forms an additional microstructure in the pores. MIP and SEM confirmed that the applied surface treatment penetrates the mortar and densifies the pore structure forming a dense membrane at the surface of the concrete. The result of the freezing-thawing resistance of coated specimens was larger than that of the non-coated ones.

Park et al. (73) applied two surface penetrants to concrete samples. The first penetrant was inorganic and had sodium silicate as the main ingredient. The second was a combination of sodium silicate and an organic polymer. These were applied to two concretes, one with a w/c of 0.55 and one with a w/c of 0.49. The samples were cured, submerged for four weeks, and then exposed to air for two weeks before surface impregnation through spraying. The surface impregnation resulted in reduced water permeability, absorption, and porosity. The inorganic penetrant resulted in concrete with slightly better resistance to chloride penetration than the combination of inorganic and organic components. This was attributed to lower viscosity and surface tension, resulting in deeper penetration depth.

Baltazar et al. (74) conducted an experimental study about the efficacy of silicate-based impregnations to protect concrete. Concrete specimens with two different water/cement ratios (0.40 and 0.70) were produced. The impregnations were evaluated with three different surface roughnesses and three different moisture contents (3.0%, 4.5%, and 6.0%). The performance of unprotected and protected concrete specimens was assessed using penetration depth, water absorption by immersion, abrasion resistance, impact resistance, and bond strength. Results show that the silicate-based impregnation effectively improved the resistance to water penetration and abrasion resistance but did not improve the resistance to impact. The reduction in water permeability was highest for the specimens to which the impregnation was applied at higher moisture contents.

Fibers

Studies have found that fibers can provide resistance to plastic and drying shrinkage cracking in concrete (75, 76, 77). Including uniformly distributed and randomly oriented short fibers in concrete significantly improves its tensile and bending strength. It allows for the bridging of forming cracks in concrete (78, 79, 80). Fibers can be readily added to concrete before or during the mixing operation. However, at higher addition dosages, the workability of the mix can be reduced significantly, and water-reducing admixtures are required to retain slump and ensure fiber dispersion.

Various types of fibers have been employed in concrete as mitigation strategies for shrinkage-caused concrete cracking. The most common and practical ones are steel and synthetic polymeric fibers. The addition of steel fibers improves the ultimate load and elastic modulus of concrete mixes and reduces the early shrinkage and cracking due to the bridging effect (81, 82). Concrete mixtures containing steel fibers exhibited

increased tension stiffening and smaller crack spacings, thus, reducing crack width compared to reference mixtures without steel fiber (83). While steel fibers rust when exposed to the concrete's surface, they appear to be more durable within the concrete mass due to a passivation layer formation in the alkaline cementitious environment (84).

Synthetic polymeric fibers used as anti-cracking admixtures in concrete have garnered tremendous attention due to their high strength, superior long-term durability, and cost-effectiveness in reducing the amount of shrinkage cracking. The mechanical blocking action of ductile polymeric fibers can inhibit the growth of microcracks in concrete due to shrinkage. The internal support system of the synthetic fibers inhibits the formation of plastic settlement cracks. The uniform distribution of fibers throughout the concrete discourages the development of large capillary channels caused by bleeding water migration to the surface, which provides locations for later-age cracking. Polypropylene (PP) fibers are the most common synthetic fibers in FRC applications due to their ability to reduce concrete autogenous and total shrinkage (85). PP embedment in concrete has been reported to reduce crack width by 62% and extend the time to cracking by 84% when the concrete specimens were subjected to restrained shrinkage (86). Other polymeric fibers, such as nylon (87) and polyolefin (86), have also demonstrated similar effects on mitigating shrinkage in concrete. However, the effectiveness of mitigation depends mainly on the distribution of fibers in concrete mixes.

Shen et al. (88) used restrained ring tests to study shrinkage in four HSC mixtures employing double hooded-end steel fibers at 0.0, 0.12, 0.24, and 0.36 percent by volume. The concrete mixtures had a w/c of 0.32. The fine aggregate was river sand, and the coarse aggregate was limestone. The measured strains in the ring tests decreased with an increasing amount of fiber, as well as the residual stress. The free shrinkage rate of HSC decreased with increasing fiber content, and the cracking potential also decreased with increasing fiber content.

Younis et al. (89) used steel fibers extracted from scrap tires in fiber-reinforced self-compacting concrete. The recycled steel fiber (RSF) lengths used were 10, 15, 25, and 35 mm. Eight mixes with various combinations of fiber lengths were considered with constant fiber content. The addition of RSF reduced the free shrinkage strain by using a single short fiber length. Increasing fiber length led to an increase in free shrinkage strain. The incorporation of RSF increased the cracking resistance. The short RSF showed better resistance to cracking than long fibers. Mixes containing long and short fibers did not exhibit cracking during the test period.

Yousefieh et al. (2017) evaluated the influence of polypropylene, polyolefin, and steel fibers on the drying shrinkage of concrete. The maximum drying shrinkage strength depended on the fibers' elastic moduli. In this regard, steel fibers have the highest elastic modulus compared to polypropylene and polyolefin fibers, resulting in the greatest increase in the tensile strength of the concrete before initial cracking. In concrete samples with a fiber content of 0.1 percent (by volume), the maximum restrained drying shrinkage strains were 72, 40, and 30 microstrains for steel, polyolefin, and polypropylene fibers, respectively. The steel fibers showed the best performance due to their hook-shaped tail. Polypropylene fibers also performed better in preventing

crack development due to their longer length and surface serrulation. All three types of fiber reduced the average crack width. The average length of cracking in fiber-reinforced concretes was more than in the control concrete, which was explained by the general behavior of fibers in producing hairline cracks. Specimens containing 0.1 percent steel, polyolefin, and polypropylene fiber (by volume) increased the cracking length by 19, 9, and 2 percent compared with the plain concrete. Adding fibers decreased the drying shrinkage cracking and delayed the initial cracking time. The first crack appears after 144 h in steel fiber reinforced concrete instead of 48 h in the control concrete.

Kawashima and Shah (90) studied fiber-reinforced concrete's early-age drying shrinkage behavior. The cellulose fibers used in this study were 100% virgin specialty cellulose fibers with an alkaline-resistant coating. They had an average length of 2.1 mm, an average diameter of 16 um, and a density of 1.1 g/cc. It was found with the w/c = 0.5 mortar that adding cellulose fibers did not reduce drying shrinkage and that the situation is similar in concrete. However, cellulose fibers effectively mitigate autogenous shrinkage of w/c = 0.28 mortar at 1% addition. And they were found to decrease crack width by redistributing wider cracks to finer cracks, of w/c = 0.44 concrete under restrained shrinkage conditions.

Aggregate Gradation

Numerous studies have shown that the common practice of using binary aggregate blends of a fine and a coarse aggregate results in a gap-graded mix with a lack of intermediate particle sizes in the 2.36 mm to 9.5 mm range. Shilstone (1990) presented a quantitative method for optimizing aggregate proportions. Shilstone's method works with the relationship between the coarseness of two larger aggregate fractions and the fine fraction, the total amount of mortar, and the aggregate particle distribution to produce an optimized blend. One of the goals of an optimized mixture is a well-graded blend of aggregates that results in a smaller paste volume. A reduced paste volume can reduce shrinkage.

Cramer and Carpenter (91) considered mixes made from aggregate gradations defined as control, near-gap, and optimized. The control mix was based on Wisconsin DOT specifications. The near-gap mix tended to have a reduced aggregate quantity in the 9.5 mm to 1.2 mm sizes with an increase in fine material. The optimized mix gradation used the principles of Shilstone (92) and practical considerations to minimize waste and had higher quantities of material in the 9.5 mm to 1.2 mm range. The near-gap mixes had shrinkage 4 to 14 percent higher than comparable control mixes. The control mixes exhibited the lowest shrinkage, and the optimized mixes did not show clear reduced shrinkage.

Ramakrishnan and Patnaik (93) evaluated optimized aggregate gradations for bridge deck concrete in South Dakota. A control mix was compared to a mix with optimized aggregate gradation through laboratory testing. The optimized mix was then used on three bridge decks in South Dakota. At 60 days, the control concrete had a drying shrinkage strain of 393 microstrains, the optimized laboratory concrete had a drying shrinkage strain of 293 microstrains, and the concrete used on the bridge decks had a drying shrinkage strain of 278 microstrains. The optimized mixture from the laboratory

and field had approximately 10 percent higher compressive strength than the control. The elastic modulus of the optimized and field concrete was also higher than the control.

Fowler and Rached (94) evaluated mixes with various sand-to-aggregate ratios to study the effect of paste volume on mix performance. They also considered using microfines to replace a portion of the paste volume. Demand for HRWRA to maintain the same slump increased with increasing sand-to-aggregate ratio and as paste volume decreased. Drying shrinkage and permeability increased with paste volume. The replacement of cement with microfines while holding the paste volume constant increased in compressive strength. Shrinkage decreased as the microfines percentage increased.

Hooten et al. (95) considered several packing models to reduce cement content while achieving the performance requirements of the Canadian Standards Association specifications. They found they could reduce the cementitious materials in typical 5080 psi (35 MPa) mixes by 8 percent and in 7250 psi (50 MPa) mixes by 16 percent while maintaining workability and air content requirements. Eight mixes achieved a drying shrinkage of less than 400 microstrains at 28 days at 50 percent relative humidity.

Henschen and Lange (96) investigated concrete mixtures designed to have high aggregate packing density that allowed a reduction in paste volume. The control mix had a paste content of 31 percent by volume and a coarse-to-fine ratio of 1.47. A second mix had a low paste content of 22 percent by volume. Two mixes were intended as paving mixtures and had paste contents of 24 and 27 percent by volume. The last three mixes all had coarse aggregate to fine aggregate ratios of 0.78. All of the mixes used a w/c of 0.42. This study demonstrated that well-graded aggregates could reduce concrete shrinkage regardless of the paste content. In addition, all the optimized aggregate mixtures showed a lower-than-expected potential for cracking compared to the control mixture. The mixtures optimized for aggregate density required significantly more water reducer to achieve desired slumps. They were workable and consolidated well with a vibrator. Reduced cement paste volume can adversely affect workability while improving the drying shrinkage and creep performance.

Ryu and Kim (97) developed a high-performance concrete paving material with lower shrinkage and reflection of sunlight. The reflectivity was reduced by including a small percentage of black pigment. Using optimized aggregate gradations for the mix design, the strength and freeze-thaw resistance of the concrete significantly improved. Incorporating fly ash at 25 percent replacement, combined with the optimized aggregate gradation, reduced the drying shrinkage. The drying shrinkage was reduced by 23 percent compared to a control mix.

Zhu et al. (98) investigated the influence of the volume and gradation of coarse aggregate on the drying shrinkage of self-consolidating concretes (SCC). An aggregate skeleton dispersion model was proposed to determine the mortar coating thickness. Based on the model and experimental results, they concluded that increasing coarse aggregate volume decreases SCC's workability and drying shrinkage. An optimum coarse aggregate volume of 33 percent was proposed. For SCC, an optimal aggregate gradation has 30 percent retained between 5 and 10 mm, 30 percent retained between

10 and 16 mm, and 40 percent retained between 16 and 20 mm for superior workability. The shrinkage of SCCs decreased with an increased volume ratio of 16 to 20 mm aggregate. The mortar coating thickness mainly influences the shrinkage of SCCs. When coarse aggregate volume is kept constant and coarse aggregate size is increased, the shrinkage of SCCs decreases with increasing mortar coating thickness because of better restraint from the coarser aggregate.

Systems in Combination

Meddah et al. (99) studied combinations of expansive and shrinkage-reducing admixtures on autogenous deformation of high-performance concrete with silica fume. The internal stress development induced during the development of autogenous shrinkage strains was investigated on three different types of HPC. HPC made with blended cement containing 10% of silica fume (SF) was used with three different water-to-binder ratios, 0.15, 0.23, and 0.30. Shrinkage-reducing agent (SRA) and an expansive additive (EXA) were combined and added to the HPC mixtures to minimize autogenous shrinkage. Using a combination of SRA and EXA resulted in a slight decrease in the compressive strength, tensile strength, and modulus of elasticity. Combining SRA and EXA reduced the autogenous shrinkage by 50% in the 0.15 mix. The autogenous shrinkage and internal tensile stress were further reduced or eliminated at higher water-to-binder ratios of 0.23 and 0.30. The reduction in shrinkage was most efficient at the higher w/b ratio. It was also found that more than 80 percent of the shrinkage develops during the first 24 hours of curing and does not increase significantly after that.

Oliveira et al. (100) presented laboratory test results of SCC's autogenous shrinkage, considering the efficiency of shrinkage-reducing admixtures, expansive binders, and the products used in combination. Nineteen concrete mixtures were considered, with six considered low strength, six considered intermediate strength, and six considered high strength. The results indicate that autogenous shrinkage was significantly reduced and sometimes eliminated by incorporating SRA and expansive products. This was found for all three strength classes of SCC studied. The risk of deleterious expansion in saturated conditions is marginal, provided the expansive products are used in appropriate dosages.

Khajehdehi et al. (101) evaluated eleven concrete mixtures with w/c ratios of 0.45 that employed lightweight aggregate for internal curing, calcium oxide-based and magnesium oxide-based SCAs, and combinations of internal curing, SCMs, and SCAs. The following conclusions were drawn:

- Internal curing provided by intermediate-sized prewetted lightweight aggregate effectively reduces drying shrinkage in concrete with moderate w/b ratios. Mixtures with IC exhibited greater early-age expansion and less shrinkage during the first 20 days of drying than companion mixes without internal curing.
- Internal curing combined with slag cement and silica fume further increased the first-day expansion and reduction in shrinkage.
- The CaO-based SCA induced a more rapid expansion of greater magnitude, with most of the expansion taking place within the first day after casting, while

the MgO-based SCA caused an expansion that steadily increased throughout the curing period and was lower in magnitude.

- When the CaO-based SCA is incorporated in a mixture containing SCMs or SCMs and IC, a larger expansion and, consequently, a lower overall shrinkage strain is observed. The increase in expansion is greater than that observed in CaO-based SCA alone or the CaO-based SCA used in conjunction with prewetted LWA. The same observation was not made for mixtures incorporating SCMs with the MgO-based SCA.

Valipour and Khayat (102) evaluated the efficiency of various shrinkage mitigation approaches in reducing autogenous and drying shrinkage of ultra-high performance concrete (UHPC). Products studied included CaO-based and MgO-based expansive agents, shrinkage-reducing admixture, and pre-saturated lightweight sand.

The incorporation of 25 percent to 60 percent pre-saturated lightweight sand decreased HRWRA demand (1.23%–1.05%) compared to the control mixture (2.3%) required to secure self-consolidating characteristics. The lightweight sand content necessary to compensate for chemical shrinkage for the investigated UHPC corresponds to 35% by volume of sand. The coupled effect of incorporating a CaO-based expansive agent with 60% pre-saturated lightweight sand resulted in significantly improved control of autogenous shrinkage of UHPC.

The coupled effect of pre-saturated lightweight sand and CaO-based expansion agent for different curing conditions indicates that increasing lightweight sand and CaO-based expansion agent replacement levels along with extending moist curing improved expansion during the moist curing period. Using shrinkage-reducing admixtures or MgO-based expansion agents combined with 60 percent pre-saturated lightweight sand effectively reduced total shrinkage by up to 30 percent. The authors suggested that the best shrinkage reduction and strength improvement performance was obtained with a mixture of 10 percent CaO-based expansion agent and 60 percent pre-saturated lightweight sand.

Shrinkage and Cracking in New Jersey and Other States

New Jersey

Sixteen high-performance concrete mixes with water-to-binder ratios ranging from 0.34 to 0.40 and varying amounts of coarse and fine aggregate were studied by Nassif et al. (103) for cracking potential. Compressive and tensile strength, elastic modulus, and unrestrained and restrained drying shrinkage were also analyzed. It was found that a higher content of coarse aggregate and a higher ratio of coarse to fine aggregates reduced cracking potential across all mixes. Silica fume use and higher cementitious material content also increased cracking potential. It was recommended that at least 1800 pounds per cubic yard of coarse aggregate be used in mixes with a coarse-to-fines ratio above 1.48. Maximum cementitious material should be limited to 700 lb per cubic yard, and silica fume should be limited to 5 percent of the cementitious component.

Oklahoma

Ramseyer and Giebler developed and used four HPC mixtures in field trials on bridge decks (104). The mixtures were developed by studying the effects of air entrainment, cementitious materials content, water to cementitious materials (w/cm) ratio, supplemental cementitious materials, fiber reinforcement, and a shrinkage-reducing admixture. The field investigation consisted of test slabs for the HPC mixtures and actual bridge construction. It was found that the shrinkage-reducing admixture had reduced unrestrained shrinkage while increasing compressive strengths but had an adverse effect on the air content. The shrinkage-reducing admixture's impact on air content was reduced by adding the admixture in small repeated doses. Moderate to low range shrinkage, high compressive strengths, and little or no cracking was achieved in the decks.

Colorado

Durham and Cavaliero (105) provided an evaluation of Colorado Department of Transportation specifications for Class H and Class HT crack-resistant concrete intended for use in bridge decks. Class H is used for bare concrete decks, and Class HT is used for deck resurfacing and repair. The shrinkage strain development rate and ultimate strain were reduced by lowering binder content and using a high dosage of shrinkage-reducing admixture while maintaining adequate development of ultimate strength at all ages. The following modifications were recommended to the CDOT specifications in place at the time of the study: 1) increase maximum allowable water-to-cement ratio from 0.42 to 0.44; 2) increase maximum allowable cement replacement with Class F fly ash from 20% to 30%; 3) incorporate the use of cement replacement with ground-granulated blast furnace slag up to 50%; 4) incorporate the use of a shrinkage reducing admixture at high dosage rates; 5) incorporate the use of a set retarder admixture at average dosage rates; 6) decrease cementitious content to 564 pounds per cubic yard when supplementary cementitious materials are not used.

Additional requirements for Class H and Class HT concrete are: 1) The concrete mix shall consist of a minimum of 55 percent sizes No. 57, No. 6, or No. 67 coarse aggregate by weight of total aggregate; 2) the cracking tendency of the laboratory trial mix shall not exhibit a crack before 15 days when tested following AASHTO T334.

Iowa

Wang et al. (106) evaluated various shrinkage components in HPC mixes used for bridge decks and overlays in Iowa. Mixes using three types of cement (Type I, I/II, IP), three supplementary cementitious materials (Class C fly ash, slag, metakaolin), and chemical admixtures (normal and mid-range water reducer, retarder, air-entraining agent) were studied. Tests were conducted for chemical, autogenous, free drying shrinkage, and restrained shrinkage, as well as creep strain, compressive strength, splitting tensile strength, and elastic modulus. The cracking potential of the concrete mixes was assessed based on the simple stress-to-strength ratio method and the ASTM C 1581 stress rate method.

It was found that autogenous shrinkage of the HPC mixes ranged from 150 to 250 microstrains, and free drying shrinkage of the HPC mixes ranged from 700 to 1200

microstrains at 56 days. This research recommends using the peak shrinkage stress-to-splitting tensile strength ratio with the consideration of concrete creep for predicting cracking potential in concrete mixes. It was also suggested that 20% Class C fly ash replacement reduced all forms of measured shrinkage. 25% ground granulated blast-furnace slag (GGBFS) replacement increased free drying shrinkage and restrained shrinkage of concrete significantly. Mixes with cement content greater than 700 lb/yd^3 showed a high potential for cracking. Mixes made with Type I cement yielded greater shrinkage than those made with Type I/II cement, which yielded greater shrinkage than those made with Type IP cement.

Mississippi

Varner (107) reports shrinkage and permeability data for thirty concrete mixtures developed as low-cracking, high-performance concrete for Mississippi. The mixtures were based on recommendations from the University of Kansas. The results indicate that Class F fly ash was more effective than Class C fly ash in reducing shrinkage, and blast furnace slag was more effective than fly ash. All three SCMs significantly reduced chloride ion permeability. Aggregate gradation optimization had less influence on length change than SCMs.

State Specifications

South Dakota

The South Dakota DOT (108) standard specifications for bridge deck preparation and resurfacing use Type I portland cement conforming to AASHTO M 85 and portland-pozzolan cement conforming to AASHTO M 240. For fly ash, Class C or F conforming to AASHTO M 295 may be used for Type I portland cement; however, fly ash may not be substituted for a portion of portland-pozzolan cement. Air-entraining admixtures for concrete shall be "one hundred percent vinsol resin based or one of the products as listed on the Department's Approved Products List for air-entraining admixtures" and shall conform to the requirements of AASHTO M 154. The chemical admixtures used shall conform to AASHTO M 194. A latex emulsion admixture is also used and is selected from a list of qualified products available on the Department's Approved Products List. The mixture proportions target an entrained air percentage of 5 ±1%, a slump of 4-8 in., a max water cement ratio of 0.40, and 60% fine aggregates. The concrete shall be between 45°F and 80°F at the time of placement and shall be maintained in this range for at least 48 hours. Traffic shall not be permitted until 96 hours after placement. A longer curing period may be required when temperatures fall below 55°F.

Colorado

The Colorado DOT (109) 2017 standard specifications include Class H concrete for bare concrete bridge decks and Class HT for bridge deck resurfacing and repair. These concretes are intended to produce decreased porosity and less cracking in the decks. The concretes have the same minimum strength of 4500 psi (31 MPa) as Class D, and DT mixes used for bridge decks, but the strength requirement does not have to be met until 56 days instead of 28 days. The cementitious requirements were reduced to 580 to

640 lb/yd3 (344 to 380 kg/m3) instead of 615 to 660 lb/yd^3 used in Class D and the minimum of 700 lb/yd3 for Class DT. Adding fly ash and silica fume and using a lower cement content reduces the permeability. The lower cement content helps reduce shrinkage cracking. Adding fly ash and silica fume also increased strength to offset the lower cement content (110). Class H and HT concrete has an air content range of 5 to 8 percent and a w/c of 0.42 to 0.44.

In the 2022 State specifications (111), Class H and HT are no longer present, while Class G was added. Class G concrete is a low-shrinkage macro fiber-reinforced concrete. The concrete mix includes macro or hybrid polyolefin fibers at a minimum dosage of 4 lbs/cy or the minimum manufacturer-specified dosage, whichever is greater. Shrinkage-reducing admixtures and expansive cement additives may be incorporated into the mix. The unrestrained shrinkage shall not exceed 0.030 percent at 28 days. When an expansive cement is used, the expansion of the laboratory trial mix shall be 0.05 to 0.09 percent at 7 days. The mix shall either have a permeability not exceeding 2,500 Coulombs at 56 days when tested following ASTM C1202 or have a surface resistivity of at least 12 kΩ-cm at 28 days using AASHTO T358. The strength requirement for Class G is 4500 psi at 28 days.

Kansas

The Kansas DOT (112) specifies the use of Moderate Permeability Concrete (MPC) for full-depth bridge decks and Low Permeability Concrete (LPC) for bridge deck overlays.

The requirements for MPC are 11.0% maximum volume of permeable voids (KT-73), 13.0 kΩ-cm minimum surface resistivity (KT-79), or 2000 Coulombs maximum from the rapid chloride permeability test (AASHTO T-277). The specifications note that concrete mixes for MPC require aggregates with a minimum soundness of 0.95 (KTMR-21), a maximum LA wear of 40% (AASHTO T 96), and a minimum acid insoluble residue of 85% (KTMR-28). These are harder aggregates with very low absorption. MPC may rely more heavily on optimized gradations, blended cements, or SCMs to meet specifications.

The requirements for LPC are a 9.5% maximum volume of permeable voids, 27.0 kΩ-cm minimum surface resistivity, or 1000 Coulombs maximum with the rapid chloride permeability test. LPC also uses harder aggregates with very low absorption. These mixes must be optimized with the MA-6 gradation. Mix designs with 5% silica fume and 95% Type I/II cement often meet the LPC requirements. These mixes have traditionally been known as silica fume concrete. Ternary mix designs help meet these requirements. Consider using 3% to 5% silica fume with 25% to 30% slag cement, or 25% to 30% slag cements with 10% to 25% Class C fly ash. Class F fly ash alone may also be effective in reducing the permeability to these levels.

Delaware

The Delaware DOT (113) has Class D concrete for structures that require 1.5 lbs of nonferrous fiber per cubic yard of concrete and shrinkage-reducing/compensating admixture. The concrete has a maximum w/cm of 0.4 and minimum compressive strength of 450 psi. The concrete can be used as deck overlays, deep cavity repairs, and approach slabs. The maximum allowable temperature for Class D concrete for

23

bridge decks is 85°F. In contrast, the maximum allowable temperature for all other concrete classes is 90°F.

CONCRETE MATERIALS

This section contains the lists of the materials and proportions used in this study. The materials are presented in two parts. The first part lists the materials and the proportions used for the intitial evaluation concrete mixtures . The second part presents the admixtures and additives used to modify the two selected mixtures used as controls for evaluation of effectiveness of the shrinkage control methods.

Initial evaluation mixture materials and proportions

Table 1 lists the materials for the intitial evaluation mixtures. The list comprises products included in the NJDOT-qualified list (at the time of testing). The list is composed of binders, aggregates, and admixtures.

There were four types of cementitious materials used. These were portland cement and three supplementary cementitious materials.

Four types of coarse aggregates with one type of fine aggregate were used in the mixtures. The coarse aggregates differ by size and gradation. The largest coarse nominal maximum size was 1 in., and the smallest was 3/8 in.. Also, one type of coarse aggregate was a lightweight aggregate, while the other three were granite.

The admixtures were an air-entraining agent, a mid-range, and a high-range water reducer.

Table 2 lists the 15 concrete mixture proportions studied for their shrinkage properties. The mixture proportions are based on approved NJDOT mixtures from different regions in New Jersey. The mixtures were selected based on their high cementitious content or low water-to-cement ratios. The highest total cementitious content in the group is 800 pcy, while the lowest water-to-binder ratio (w/b) is 0.34.

Table 1 - Concrete materials for concrete mixtures

Material	Type/Product	Manufacturer
Binders		
Portland cement	Type I	Lehigh Cement
Fly ash	Class F	Separation Tech.
Ground granulated blast furnace slag (GGBFS)	Grade 100	Lehigh Cement
Silica fume	Rheomac SF100	Master Builders
Aggregates		
Coarse aggregate #57	granite	Hanson Aggregates
Coarse aggregate #67	granite	Hanson Aggregates
Coarse aggregate #8	granite	Hanson Aggregates
Coarse aggregate #8 (LWA)	lightweight agg	Northeast Solite
Fine aggregate	concrete sand	Hanson Aggregates
Admixtures		
Air entraining admixture (AEA)	Sika Air	Sika
Mid-range water reducer (WR)	Sikament 475	Sika
High-range water reducer (HRWR)	Sikament 686	Sika
Retarder	Sikatard 440	Sika

Table 2 - Concrete mixtures

MIXTURE ID	Region	Class	Coarse Aggregate				Fine Aggregate	Portland Cement	Fly Ash	GGBFS	Silica Fume	Water	Air Entrainer	Water Reducer	HRWR	Retarder
			#57	#67	#8	#8 LWA										
			lb/yd^3										oz/yd^3			
NEABR200991	North	HPC-1	-	-	1508	-	1244	600	100	-	25	290.6	8	-	36.25	14.5
NEABR201093	North	HPC-1	1782	-	-	-	1083	570	130	-	25	290.6	2.9	-	36.25	14.5
NCCNA335350	North	HPC-1	-	-	1650	-	1230	455	-	320	25	320.6	0.25-4	2-4	8-24	2-4
NCCNA335391	North	HPC-1	1800	-	-	-	1201	395	-	263	-	263.9	0.25-4	2-4	8-24	2-4
NCCNA335392	North	HPC-1	1800	-	-	-	1194	370	-	263	25	263.9	0.25-4	2-4	8-24	2-4
NCTEO200859	North	HPC-1	1440	-	360	-	1140	400	-	260	25	274.7	11.2	19.8	92.4	-
NSPSP201098	North	HPC-1	1818	-	-	-	1158	505	130	-	25	264.7	10.53	-	85.7	-
NSRWA200992	North	HPC-1	1819	-	-	-	1138	555	100	-	25	273.0	1.7	-	81.6	-
Class P2	Central	Class P2	-	-	-	820	1400	800	-	-	-	272	a.n.*	-	a.n.*	-
Class P-X	Central		-	1810	-	-	1292	570	-	135	-	256	a.n.*	-	a.n.*	-
Class P	Central	Class P	-	1720	-	-	1035	640	160	-	-	272	a.n.*	-	a.n.*	-
HPC-1	Central	HPC-1	-	1834	-	-	1253	435	-	240	25	250	a.n.*	-	a.n.*	-
B Slip Form	South	Class B	-	-	1660	-	1319	500	110	-	-	298.1	-	-	-	-
A w/hr	South	Class A	1650	-	-	-	1255	525	-	175	-	280.6	-	-	-	-
HPC Type 1	South	HPC-1	1735	-	-	-	1180	570	130	-	25	298.1	-	-	-	-

*as needed
HPC-1   verification strength: 5400 psi @ 56 days (114)
Class A   verification strength: 5400 psi @ 28 days (114)
Class B   verification strength: 4500 psi @ 28 days (114)
Class P   verification strength: 6000 psi @ 28 days (114)
Class P2 verification strength: 7000 psi @ 28 days (114)

Shrinkage control admixtures and additives

The shrinkage control admixtures and additives are listed in Table 3. Five types were included in the study.

The shrinkage-reducing admixture (SRA) has both shrinkage-reducing and shrinkage-compensating capabilities. This was mentioned in the manufacturer's product description and indicated by having sodium hydroxide (for reducing) and magnesium oxide (for compensating) in the admixture. However, the shrinkage-compensating admixture (SCA) used in the study does not indicate a shrinkage-reducing capability. Both admixtures are in powder form and are added to the mixture during the mixing process.

The internal curing additive is a fine lightweight aggregate. It is incorporated in concrete mixtures as a partial replacement for fine aggregate. A portion of the concrete sand that was volumetrically equal to the volume of LWA required for internal curing was removed and replaced with the LWA.

Two coatings were tested for their effects on shrinkage. Both materials are primarily intended to fortify concrete surfaces for abrasion and wear. One coating is lithium silicate-based (LS), and the other is a polymer-modified cementitious paste (EN). LS is a concentrated liquid that is diluted in water when applied to hardened concrete. It was applied to small samples (prisms and cylinders) by submerging them in the solution while the concrete rings were sprayed. (Sample types are described in the Concrete Tests section.) EN was prepared based on the manufacturer's instructions and was brushed on samples.

The synthetic fibers are 2 in. long with an aspect ratio of 75. They have specifically been designed to replace welded wire reinforcement, steel fibers, and light rebar reinforcement. The fibers are added to the mixture during the concrete mixing. The fibers are shown in Figure 1.

The dosages applied to control mixtures are given in Table 4. The SRA and SCA dosages are the maximum and half of the manufacturer's recommended dosages. The LWA dosages are the calculated required amount based on the work of Bentz and Weiss (115) and half of the calculated amount. The LS dosage is based on the manufacturer's recommendation. The EN dosage is the average amount of a single-layer coat applied to prism specimens. The fiber dosage is half of the maximum recommended dosage by the manufacturer. The maximum dosage of fibers will require a modification of the proportions of the control mixture.

The two control mixtures were selected based on the shrinkage test results, which are discussed in the following sections.

Table 3 - Shrinkage control admixtures and additives

Type	Material	Product	Manufacturer
Shrinkage Reducing Admixture (SRA)	Magnesium oxide, Ethanol, Sodium hydroxide	Control NS	Sika
Shrinkage Compensating Admixture (SCA)	Magnesium oxide	Control SC	Sika
Internal Curing (LWA)	Fine lightweight aggregate, expanded shale	Hydrocure	Northeast Solite
Coating (LS)	Lithium silicate	Lithi-Tek 4500	Kretetek Industries
Coating (EN)	Polymer modified cement	Endurablend	Pavement Surface Coatings
Fiber	Polypropylene and polyethylene blend	STRUX BT50	GCP

Table 4 - Dosages of shrinkage control admixtures and additives

Type	Control mixture that is modified	Dosages	
Shrinkage Reducing Admixture (SRA)	NCTEO200859	24 lb/yd^3	48 lb/yd^3
Shrinkage Compensating Admixture (SCA)	NCTEO200859	24 lb/yd^3	48 lb/yd^3
Internal Curing (LWA)	NCTEO200859	238* lb/yd^3	476* lb/yd^3
Coating (LS)	Class P	1:2 water	-
Coating (EN)	Class P	0.66 lb/ft^2	-
Fiber	NCTEO200859	7.5 lb/yd^3	-

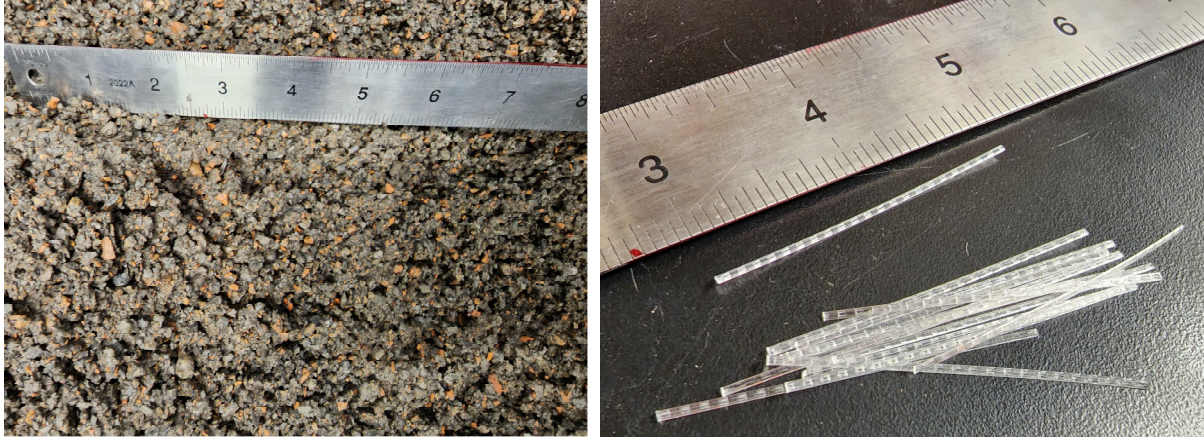*Values are dry weight; however, mixed in concrete saturated surface dry.

Figure 1. LWA (left) and fibers (right)

Calculation of LWA dosage: The following equations refered from (115) equate the water demand of the mixture with the water supply that can be obtained from the LWA to help calculate the theoretical amount required to overcome chemical shrinkage completely:

$$C_f \times CS \times \alpha_{max} = S \times \Phi_{LWA} \times M_{LWA} \tag{1}$$

$$M_{LWA} = \left(C_f \times CS \times \alpha_{max}\right) / \left(S \times \Phi_{LWA}\right) \tag{2}$$

where C_f = binder factor, CS = chemical shrinkage of binder at 100% reaction, α_{max} = degree of hydration, S = saturation level of LWA, Φ_{LWA} = sorption capacity of LWA, and M_{LWA} = dry weight of LWA. An "IC - Max" condition uses the M_{LWA} calculated from this equation, while an "IC - Half Max" uses half that value.

For the fiber-modified mix, only half of the dosage recommended by the manufacturer was tested. There was an attempt to prepare a mix with the full recommended dosage (15 lb/yd^3), but the workability was very poor. Even after adding superplasticizer over the maximum dosage of 18 fl.oz. per 100 lb of binder, as recommended by the manufacturer, the target slump was not achieved (the slump was nearly zero), and the mix started showing signs of segregation. Therefore this mix was omitted from further testing.

CONCRETE TESTS

Overview of tests

Fifteen mixtures were first tested to evaluate their shrinkage behavior. The shrinkage tests were autogenous shrinkage, drying shrinkage, and restrained ring shrinkage cracking. Based on the results of the tests, two control mixtures were selected for modification with shrinkage control admixtures and additives. The modified mixtures were then tested for the effects of the admixtures and additives on autogenous shrinkage, drying shrinkage, and restrained shrinkage. The compressive and tensile strength, elastic modulus, and creep of the modified mixtures were also measured. .

The modified mixtures were also tested for electrical resistivity and resistance to cyclic freezing and thawing to evaluate their durability. Finally, slabs made from modified mixtures were exposed to field conditions to measure their shrinkage behavior.

The sections below describe the details of the different tests conducted on the control and modified mixtures.

Shrinkage tests (Autogenous, drying, and restrained shrinkage)

The autogenous shrinkage tests of concrete were conducted according to ASTM C157 (116). Three 3x3x11¼ in. specimens were cast and demolded after 24 hours for each concrete mix. Immediately after de-molding, the surfaces of the specimens were sealed with aluminum tape, paraffin wax, or bitumen. After sealing, the initial length was measured, and the specimens were kept in a room at T=23±2 ºC. The specimens' length changes were measured with a length comparator for up to 28 days.

The free-drying shrinkage tests were also carried out according to ASTM C157. Specimens were also three 3x3x11¼ in. prisms that were cast and then de-molded after 24 hours. Unlike the autogenous test, the specimens were not sealed but were cured for 6 days in lime-saturated water after demolding. The specimens were then subjected to drying at RH=50±4% and T=23±2°C. The specimens' lengths were measured for up to 28 days. It is noted that ASTM C157 requires specimens to be cured for 28 days and dried for 448 days. Due to the limited project time, the short time of moist curing (7 days) and shrinkage measurements was employed in the study. Since all specimens were cured in the same manner, the test results were used for a comparative study.

The shrinkage cracking potential of concrete was determined by the restrained ring tests according to ASTM C1581 (117). In the test, three specimens were cast for each concrete mix. One day after casting, the specimens were de-molded by removing the outer ring. The top surfaces of the ring specimens were then coated with paraffin wax or bitumen. The specimens were then subjected to the same drying condition (RH=50±4% and T=23±2°C) as the free drying shrinkage tests. While shrinking, the concrete exerts pressure on its inner steel ring. Therefore, the strains of the steel ring were measured immediately after casting by attached strain gages. The strain gages record strain every 10 minutes until the tested ring cracks or reach 28 days.

Hardened Concrete tests (Compressive and tensile strength, modulus, creep)

The compressive and splitting tensile strength and elastic modulus were determined from 4 in. x 8 in. concrete cylinders at 7, 28, and 56 days. The test methods were based on ASTM C39 (118), C496 (119), and C469 (120), respectively. Three specimens were cast for each type of test and each test day. All the specimens were cured in lime-saturated water until the testing day.

The creep testing was conducted following ASTM C512 (121). Two 4 in. x 8 in. concrete cylinder specimens were tested in creep, and a third 4 in. x 8 in. control cylinder was monitored simultaneously for shrinkage. The concrete specimens were first cured for 28 days in lime-saturated water. After curing, two cylinders were loaded to up to 40% of the compressive strength at the loading age and maintained throughout the test period. Concrete deformation readings for the loaded cylinders were taken before

and after loading, at 2 to 6 h later, then daily for 1 week, weekly until the end of 1 month, and monthly until the end of 6 months. Length change readings from the control cylinders were also recorded. The deformations were measured using a demountable strain gauge. The specimens under load were kept in the same room as the drying shrinkage specimens.

Figure 2. Creep frame with specimens under load

Durability Tests (Resistivity and Resistance to Cyclic Freezing-Thawing)

Surface resistivity tests were measured on 4 in. x 8 in. concrete cylinders at ages 7, 28, and 56 days following AASHTO T358 (122). Three specimens were tested on each testing day. The measurements were made at quarter points on the side of the cylinders. The results are reported as the average of all the readings from all specimens.

The resistance of concrete to cyclic freezing-thawing was measured following ASTM C666 (123). Three 3 in. x 4 in. x 16 in. prisms were prepared for each mixture type. The specimens were cured for 14 days in lime-saturated water before the cyclic freezing and thawing.

Field exposure

To study the performance of the shrinkage cracking mitigation techniques and materials on New Jersey concrete and climate, mixtures were tested by casting restrained slabs in the field and making observations. The restrained slabs' geometry and restraint were based on the recommendations of ASTM C1579.

The shrinkage was measured using an externally mounted vibrating wire placed in the middle of the slab. The vibrating wire recorded the strain of the concrete every 5

31

minutes. Two slabs were cast per mixture type tested.

RESULTS

Initial evaluation mixture shrinkage

The measured autogenous and free drying shrinkage, by percent of length changes, in the initial fifteen mixtures are plotted in Figure 3 and Figure 4. The range of autogenous shrinkage is 0.026% to 0.052%. The mixture with the largest autogenous shrinkage is NCTEO200859. On the other hand, the range of drying shrinkage is 0.011% to 0.086%. The mixture with the largest drying shrinkage is Class P. The values of autogenous and drying shrinkage at 28 days for the initial evaluation mixtures are provided in Table 6.

The correlations of the initial evaluation concrete mixture components with autogenous shrinkage and free drying shrinkage were calculated using the statistics software JMP. In this analysis, mixtures B Slip Form and Class P2 were excluded. This is because B Slip Form has a w/b (0.49) that is much higher than the other initial evaluation mixtures, while Class P2 has lightweight coarse aggregates. The parameters considered are the amounts of portland cement, total binder, water, fine aggregate, coarse aggregate, and w/b. The results of the correlation calculations are tabulated in Table 5. A positive value means increasing the parameter also increases shrinkage, and a negative correlation value means increasing the parameter decreases shrinkage.

The correlation values are relatively low or not close to 1. This is because the mixtures considered were not parametrically designed, i.e., one parameter value is varied while others are maintained. Instead, the mixtures represent NJDOT-approved concrete mixtures with high cementitious content and low w/b.

The correlation values indicate that the parameter influencing autogenous shrinkage of the mixtures is the amount of aggregates. The increase of fine aggregate or decrease of coarse aggregates tends to increase autogenous shrinkage. On the other hand, the increase in portland cement and total binder while decreasing the amount of fine and coarse aggregates tends to increase the drying shrinkage.
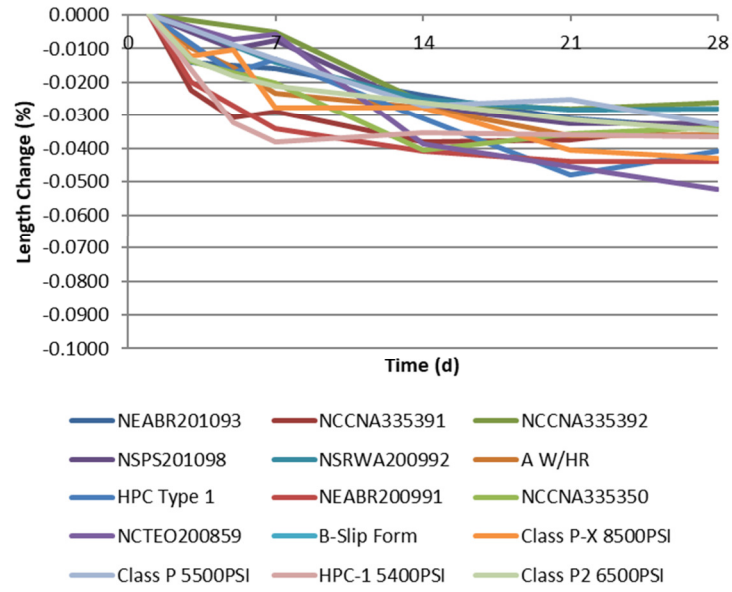
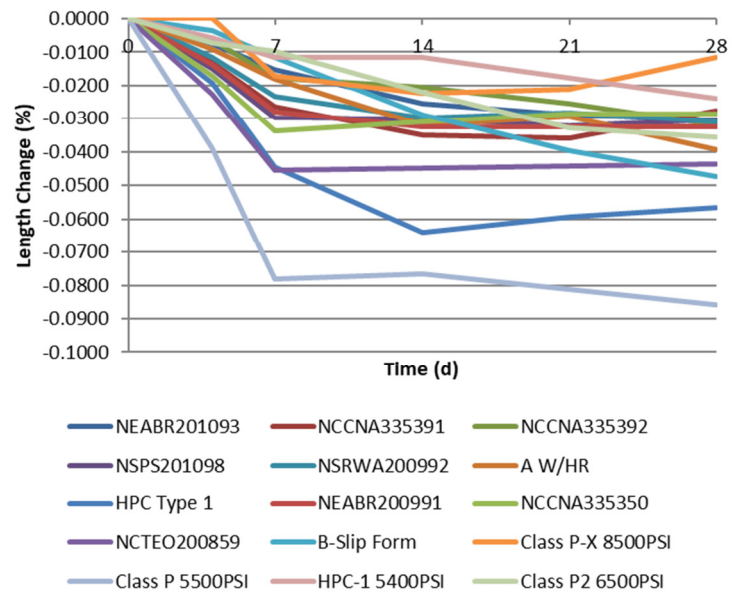Figure 3. Length change of prisms due to autogenous shrinkage

Figure 4. Length change of prisms due to drying shrinkage

33

Table 5 - Correlation of autogenous and drying shrinkage to the initial evaluation concrete composition

	Portland Cement	Total Binder	Water	w/b	Fine Aggregate	Coarse Aggregate
Autogenous Shrinkage	0.0846	0.0831	0.0882	-0.0074	0.2227	-0.2337
Free Drying Shrinkage	0.3938	0.4990	0.1981	-0.2762	-0.6806	-0.2015

The plots of the strains over time that were obtained from the restrained ring tests are in Figure 5. The end of the curves indicates the completion of the test for the specimen, which is either when the concrete ring cracks or it reaches 28 days without cracking. Based on the strain curves, the average age at cracking and average stress rate were calculated following ASTM C1581. The calculated results are tabulated in Table 6. Also, based on ASTM C1581, the potential for cracking for each initial evaluation mixture type was determined. The potentials for cracking of the mixtures ranged from moderate-low to high and are listed in Table 6. Of the mixtures tested, three mixtures were identified as having a high potential for cracking. The ring specimen of these mixtures cracked within seven days of the casting of the rings.
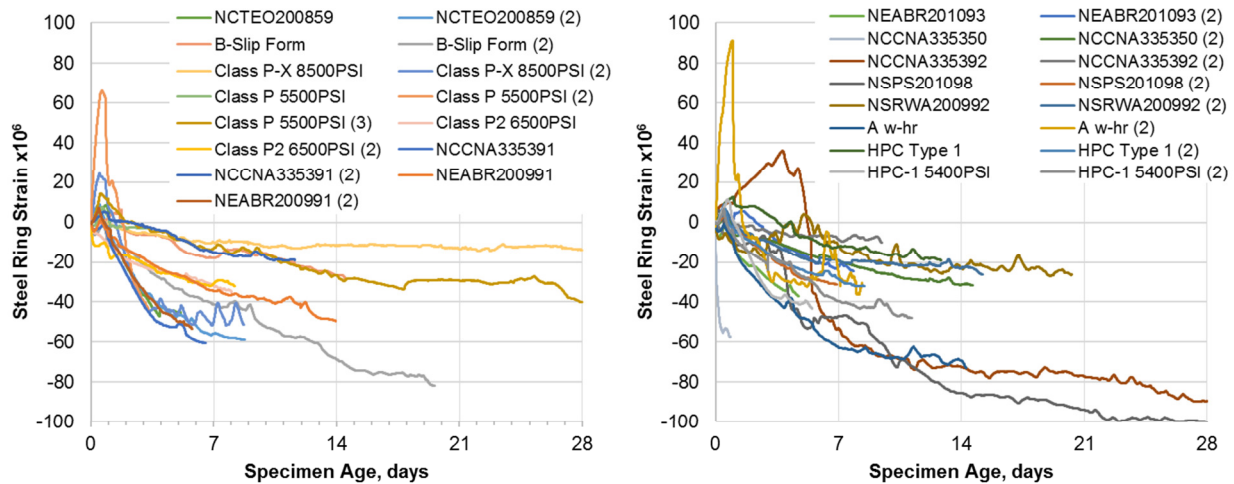

Figure 5. Steel ring strain due to concrete ring shrinkage

Table 6 - Restrain, drying, and autogenous shrinkage results

	Autogenous Shrinkage	Free Drying Shrinkage	Restrained Shrinkage		
	28-d Length Change (%)	28-d Length Change (%)	Average age at cracking (D)	Average stress rate (MPa/D)	Potential for Cracking
NSRWA200992	-0.0280	-0.0310	18	8.7	Mod-Low
HPC Type 1	-0.0410	-0.0567	17	14.5	Mod-Low
B Slip Form	-0.0510	-0.0472	17	18.9	Mod-Low
A w/hr	-0.0360	-0.0393	17	20.3	Mod-Low
NCCNA335391	-0.0330	-0.0277	15	36.3	Mod-Low
NCCNA335392	-0.0260	-0.0320	9[a]	16.0	Mod-Low*
NCCNA335350	-0.0337	-0.0287	8	14.5	Mod-High
HPC-1	-0.0367	-0.0240	14	18.9	Mod-High
Class P2	-0.0347	-0.0357	8	21.8	Mod-High
Class P-X	-0.0430	-0.0117	9[a]	27.6	Mod-High*
NSPSP201098	-0.0325	-0.0303	7[a]	30.5	Mod-High*
NEABR200991	-0.0440	-0.0326	10	46.4	Mod-High
NCTEO200859	-0.0523	-0.0437	7	65.3	High
NEABR201093	-0.0340	-0.0307	6	37.7	High
Class P	-0.0330	-0.0860	3	72.5	High

a – one ring did not crack; * - based on stress rate

The mixtures with the highest cracking potential, free drying shrinkage, and autogenous shrinkage were considered to select the mixtures to be modified with shrinkage control admixtures and additives. NCTEO200859 was selected to be modified with SCA, SRA, LWA, and fibers because of the high values of the results. On the other hand, Class P was selected to be modified with coatings because of the high cracking potential but a lower value of autogenous shrinkage.

Effects of SRA, SCA, IC, coating, and fiber on concrete with high shrinkage cracking potential

The autogenous shrinkage measurements of modified mixtures and the control mixtures are presented in Figure 6 and Figure 7. Half of the recommended dosage of SRA had less shrinkage than the control at a later age, while using the maximum recommended dosage reduced the shrinkage from an early age. The LS and EN application reduced shrinkage, but SCA modification did not reduce the autogenous shrinkage.

Fibers, even at a dosage of half the recommended, helped reduce autogenous shrinkage by 36%. However, the LWA internal curing agent, when used at the maximum dosage, led to the best performance by reducing the shrinkage at 28 days to 0.008%, which is a 64% reduction from the control sample. When used at half the maximum dosage, the LWA decreased shrinkage to a lesser extent, as expected.
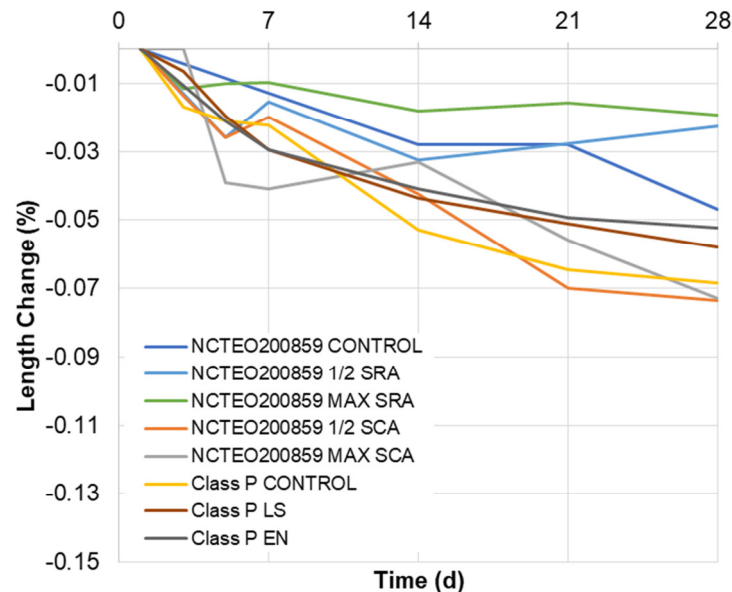

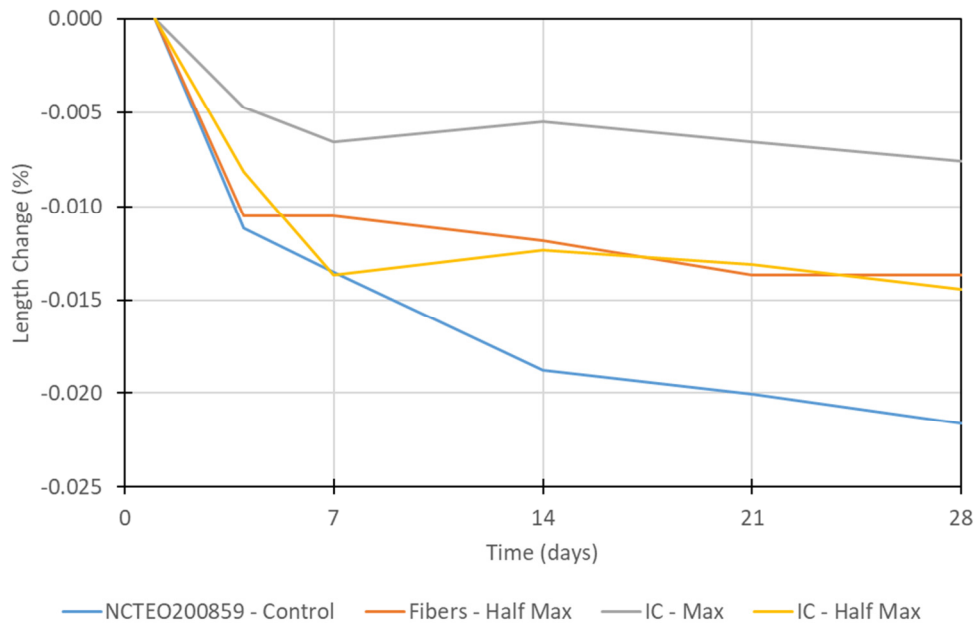Figure 6. Length change of control and modified mixtures due to autogenous shrinkage – SCA, SCA, LS, EN

Figure 7. Length change of control and modified mixtures due to autogenous shrinkage
– Fibers, IC

Figure 8 and Figure 9 contain the length changes of control and modified mixtures due to drying shrinkage. Adding SRA, either half or the maximum of the recommended dosage, reduced drying shrinkage by about the same degree. For SCA, using the maximum dosage reduced drying shrinkage, but only half the maximum dosage did not change the shrinkage. For the coatings, LS did not affect shrinkage, but EN reduced drying shrinkage slightly.

In Figure 9, while the effect on autogenous shrinkage of LWA and fibers was obvious, the effect on free-drying shrinkage was inconclusive. The control and the mix with fibers showed similar behavior throughout the test period. The mixes with LWA (at both max and half max) showed higher drying shrinkage by 21 days. Therefore the results indicate that although LWA decreased the autogenous shrinkage of this mix, especially at max dosage, they do not exhibit the same apparent benefit on drying shrinkage.
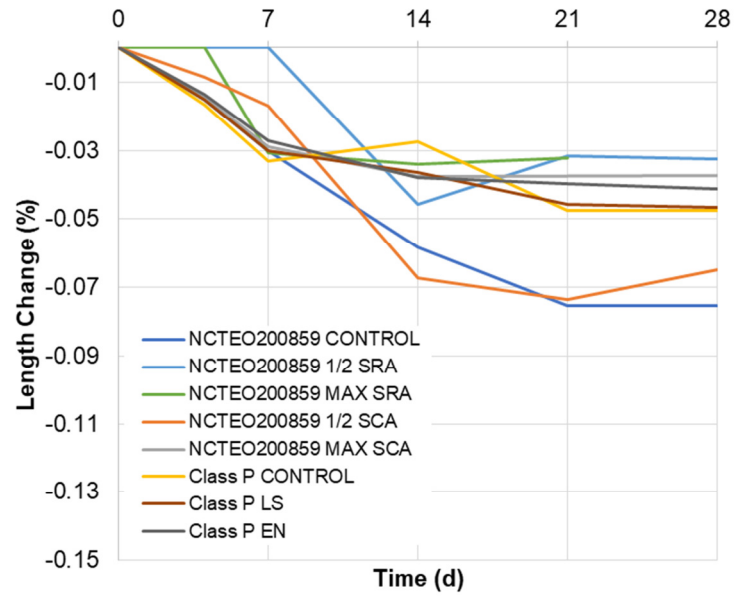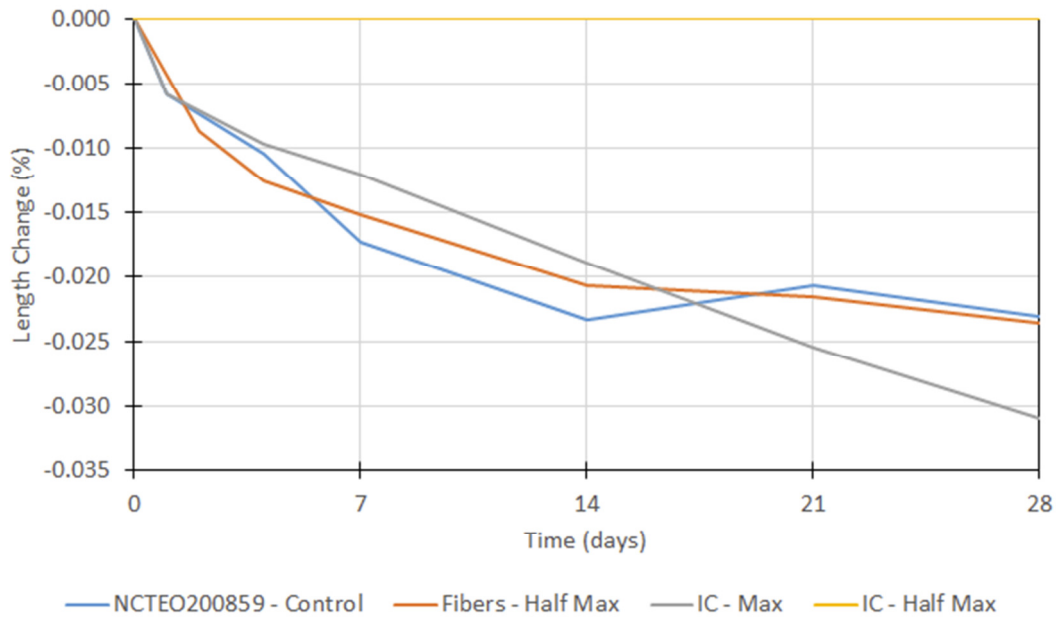
Figure 8. Length change of control and modified mixtures due to drying shrinkage –
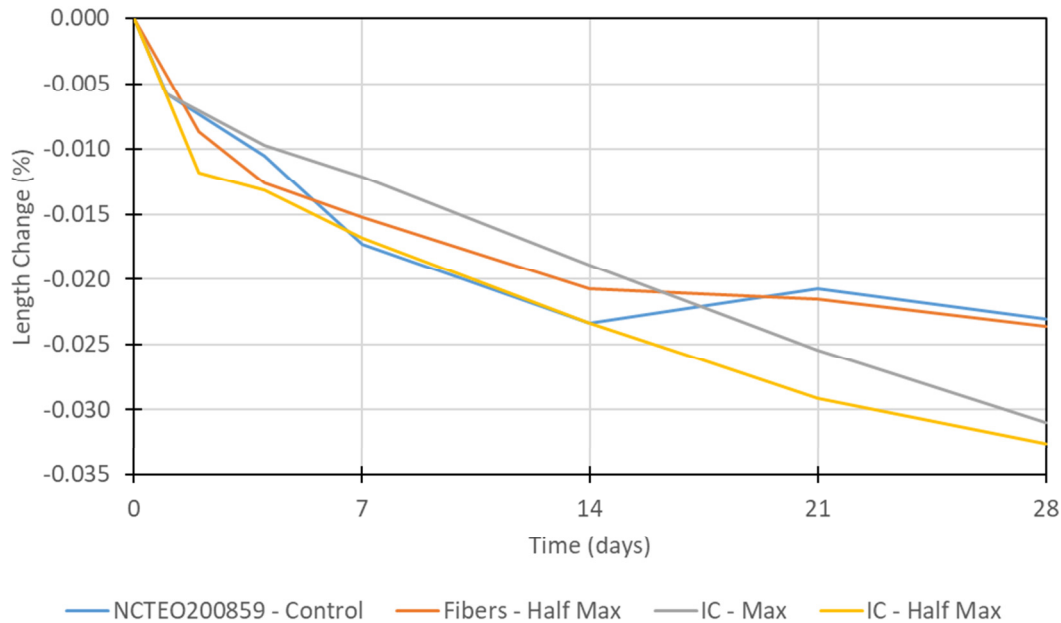SCA, SCA, LS, EN

Figure 9. Length change of control and modified mixtures due to drying shrinkage – Fibers, IC

The restrained ring shrinkage results of modified mixtures are presented in Figure 10 and Figure 11. In Figure 10, the development of strains in the rings with SRA was similar regardless of dosage. However, the concrete rings did not crack in either half or maximum dosages during the testing period. One ring specimen did not crack for the rings with SCA, while others cracked even with the maximum dosage. The SCA can reduce shrinkage and cracking potential based on the drying and restrained ring shrinkage test results. However, the dosage, mixture processing, and compatibility with the concrete materials require further investigation to optimize the use of the SCA for cracking potential reduction.

In Figure 11, both fibers and LWA were effective in reducing the total shrinkage on day 28. Based on the results from the prism tests, most of the reduction in shrinkage can be attributed to the reduction in autogenous shrinkage. However, the results are inconclusive in dictating which shrinkage reducing measure is more effective for the mixture tested.
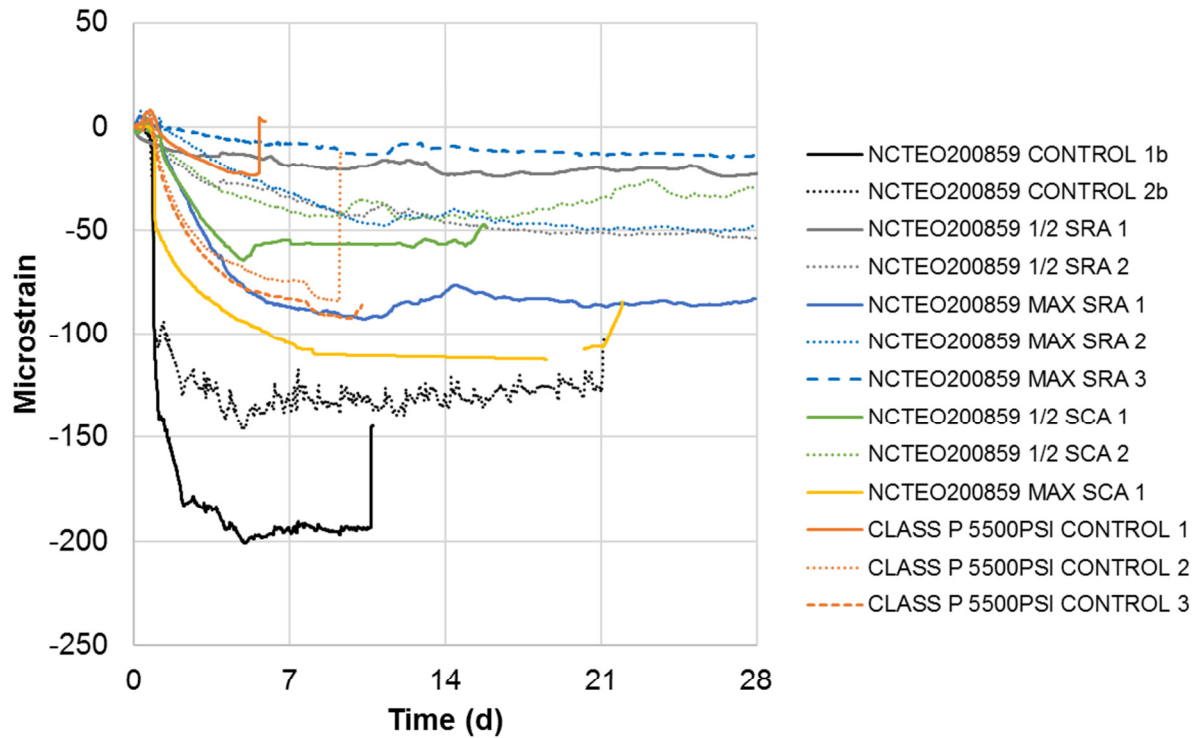
Figure 10. Steel ring strain due to control and modified concrete ring shrinkage – SCA, SCA
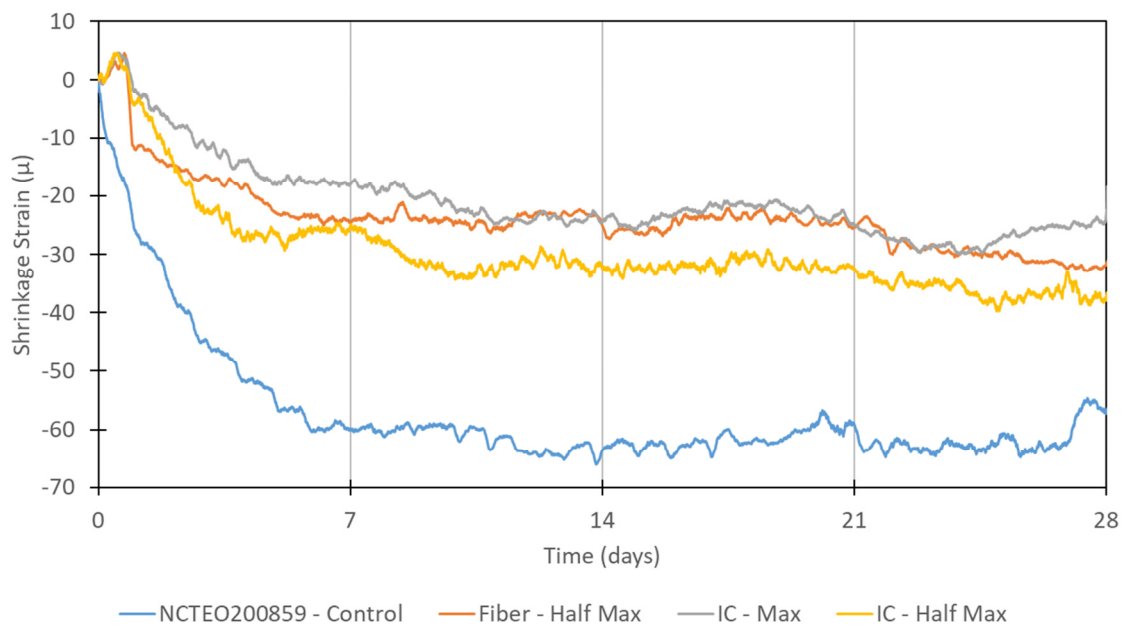

Figure 11. Steel ring strain due to control and modified concrete ring shrinkage – Fibers, IC

40

Effects of shrinkage prevention techniques and materials on other concrete properties

The compressive strengths of the modified mixtures are shown in Figure 12. The modified NCTEO200859 had higher strengths compared to the control. For the modified Class P mixtures, the strengths were higher than the control at 28 days but were lower at 56 days. However, all modified Class P mixtures had strengths higher than the required verification strength of 6000 psi.

For the splitting tensile strength results shown in Figure 13, the modified NCTEO200859 mixtures were higher than the control at 28 days but lower at 56 days. The modified Class P mixtures were lower than the control at 28 and 56 days. However, all mixture tensile strengths were greater than 600 psi at 28 days and 700 psi at 56 days.

The elastic modulus results are plotted in Figure 14. The moduli of the mixtures at 28 and 56 days were similar to the controls, ranging from 3550 ksi to 4850 ksi, except for the mixtures with fiber and maximum dosage of SRA. The mixtures with fibers and maximum dosage of SRA had moduli of 5000 to 5300 ksi.
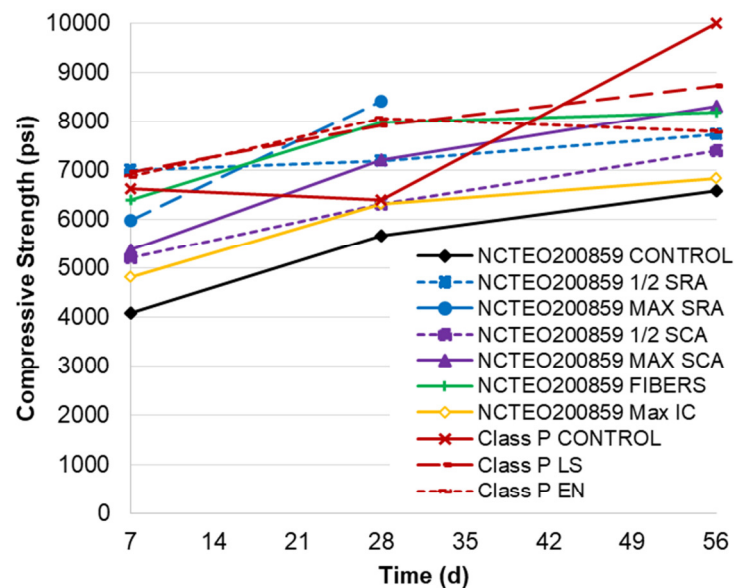

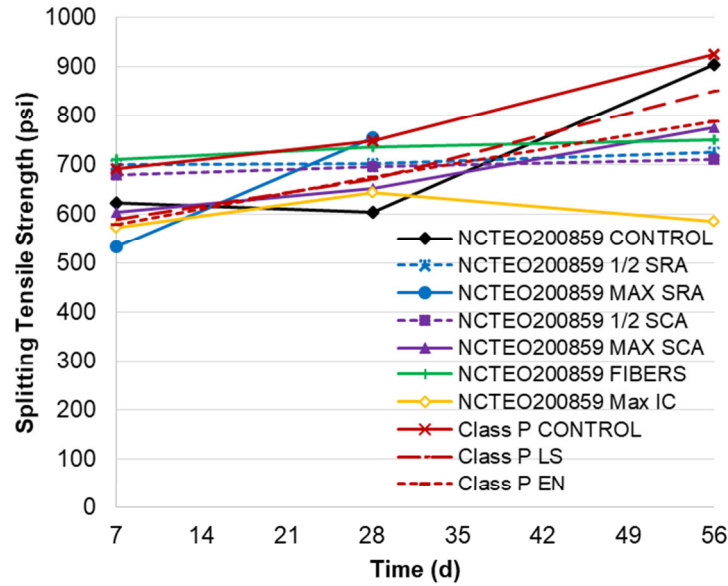Figure 12. Compressive strength of the modified mixtures

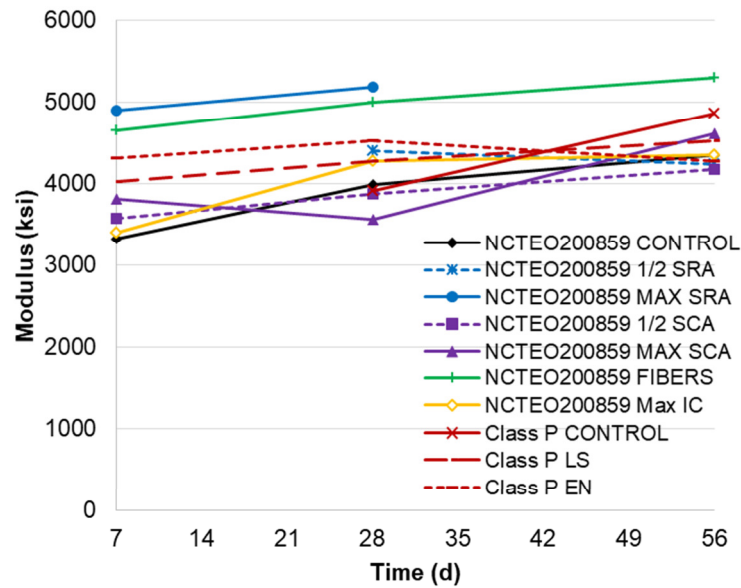Figure 13. Splitting tensile strength of the modified mixtures

Figure 14. Elastic modulus in compression of the modified mixtures

The results of the creep tests for the SCA-modified mixtures are plotted in Figure 15. The deformations of the creep specimens and control cylinder were recorded for up to 125 days. Then, the total strains per unit stress were calculated as the difference between the results from the loaded specimens and the control cylinder, divided by the stress on the loaded specimens. The strains per unit stress were then plotted on a semilog scale, in which the logarithmic axis was time, as shown in Figure 15. The creep

rate is the slope of the regression line on the creep curve. Based on the results, the SCA does not significantly impact creep since the creep rates of the SCA-modified mixture is similar to the control.
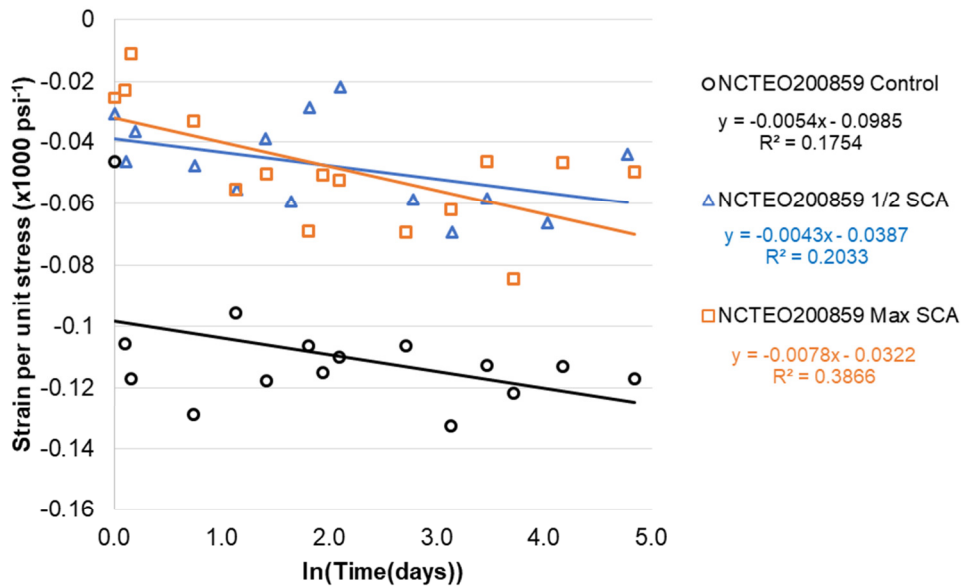

Figure 15. Creep test result of the modified mixtures

The results for the resistivity of the mixtures are plotted in Figure 16. The surface resistivity of the mixture with fibers and LWA was calculated from bulk resistivity results using the relationship given in (124). Modified mixtures with LS, EN, IC, and fibers had resistivity lower than 19 kΩ-cm (acceptance requirement for HPC in 114). All other mixtures had resistivities greater than 19 kΩ-cm. The likely causes for the low resistivity are the conductivity of lithium for LS, possible porosity between the concrete and the EN coating, and the possible porosity increased by adding fibers and LWA. The EN coating was brushed on the surface of newly demolded concrete specimens. Hence, specimen surface preparations and coating application methods can be investigated to improve the interface between the coating and the concrete. Also, the fibers were added to the concrete mixture without modifying the proportions. Therefore, adjusting the mixture proportions to accommodate the stiff fibers will likely improve the resistivity.

The results for the cyclic freeze-thaw durability of modified mixtures with SRA and SCA are shown in Figure 17. The relative dynamic modulus (RDM) is computed following ASTM C666. All the RDM results were greater than 80%, which is the requirement for HPC (114). The results indicate that with air entrainment, the admixtures do not affect concrete's durability to cyclic freezing and thawing.
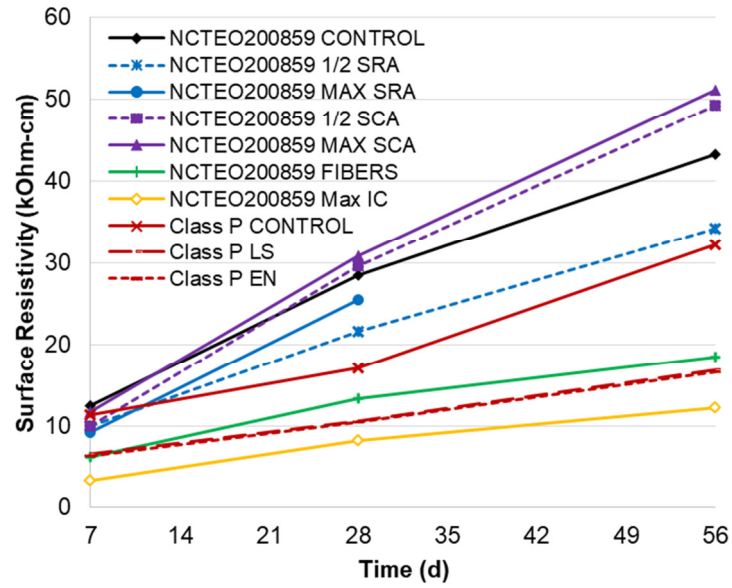
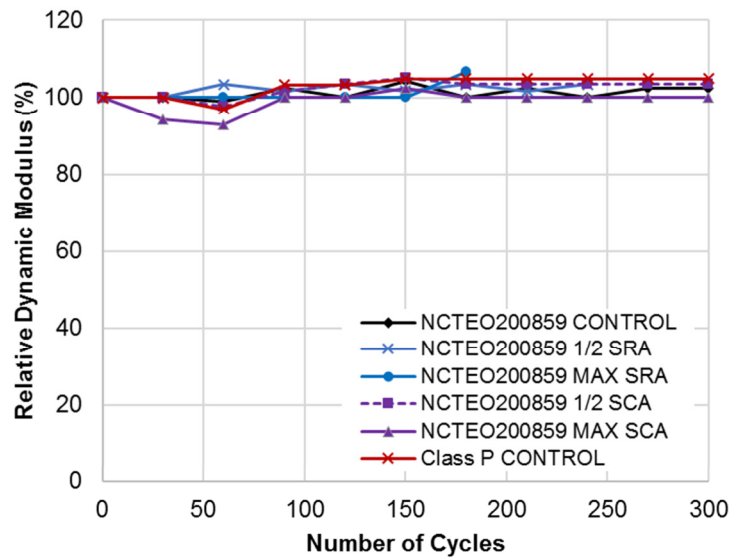Figure 16. Surface resistivity of the modified mixtures

Figure 17. Relative dynamic modulus of specimens subjected to cyclic freezing and thawing
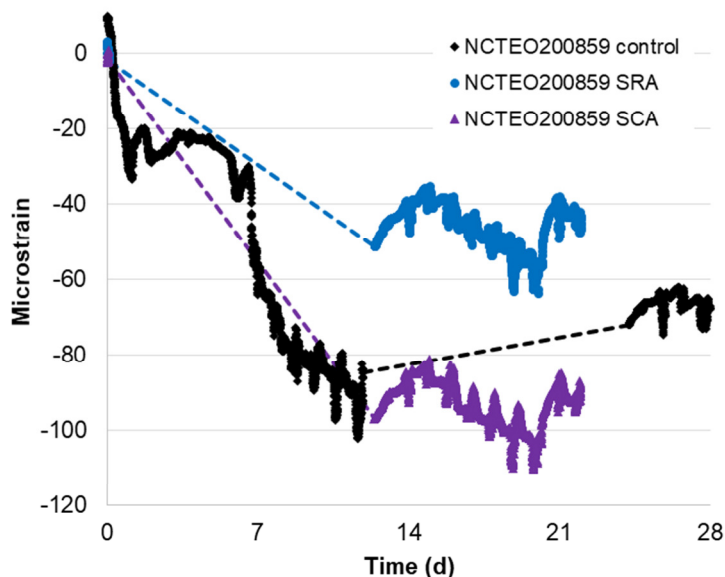
44

Figure 18 – Concrete slabs with top-mounted strain gauges (left) and slab strains over time (right)

The slabs tested in the field and the average strains of the slabs are shown in Figure 18. The dash lines in the plots connect the gap in data that was lost in the data logger. The recorded shrinkage strains in the slabs had reached 100 microstrains for the control mixture NCTEO200859 and the modified mixture with SCA. However, the modified mixture with SRA had only shrunk by 60 microstrains, demonstrating its robustness under field exposure. Further field testing can be performed on the other mitigation measures, LWA, fibers, and coatings, to study their robustness in the field.

CONCLUSIONS

Control mixtures with high cementitious content and low w/b ratios, as well as various materials that can be used to reduce shrinkage and mitigate cracking, were studied. The following conclusions are derived from the study:

1. The cracking potential of control mixtures ranged from moderate-low to high. Control mixtures with high cracking potential are restrained rings that crack within seven days of casting.
2. Control mixture autogenous shrinkage increases with the increase of fine aggregate and decrease of coarse aggregates. On the other hand, the increase in portland cement and total binder while decreasing the amount of fine and coarse aggregates tends to increase the drying shrinkage.
3. The shrinkage-reducing admixture, SRA, effectively reduced the concrete's shrinkage and cracking potential.
4. The shrinkage compensating admixture, SCA, did not reduce the autogenous

shrinkage of the concrete but reduced the drying shrinkage when the maximum dosage was used. Adding SCA to the concrete extends the craking time. And in one sample, the concrete did not crack after 28 days with only half the recommended dosage.
5. The cementitious coating, EN, slightly reduced autogenous and drying shrinkage.
6. The lithium silicate, LS, reduced the autogenous shrinkage but not the drying shrinkage.
7. The internal curing agent, LWA, reduced the autogenous shrinkage but not the drying shrinkage. LWA also reduced the restrained ring cracking potential.
8. The fibers reduced the autogenous shrinkage but did not reduce the drying shrinkage. The fiber also reduced the restrained rings cracking potential.
9. SRA, SCA, fibers, LS, and EN do not adversely affect concrete's strength and elastic modulus.
10. SRA reduced surface resistivity, while SCA did not. Fibers, EN, and LS, reduced surface resistivity. Lithium silicate is conductive and may reduce resistivity. No modification was made to the mixture proportions to accommodate the addition of the fibers. EN was brushed on the surface of the concrete immediately after demolding.
11. SRA was more robust than SCA in reducing shrinkage when exposed to field conditions.

RECOMMENDATIONS

To mitigate cracking in concrete by using admixtures and additives, the standard restrained ring test ASTM C1581 can be adopted for evaluating the concrete's performance after modification. A mixture with a low cracking potential classification based on the test has a lower risk of concrete cracking due to shrinkage. However, it was observed that the cracking age in a restrained ring test could greatly vary, even for specimens from the same batch. It is therefore recommended that specifications for concrete shrinkage cracking be met by three specimens from the same batch to be approved. This will reduce the risk of failures due to incompatibility, processing, and testing. Such a specification can be in the form of

Table 7 - Recommendation on the potential for cracking requirement

Design and Verification Requirements for HPC

Performance Characteristic	Test Method	Requirements	
		HPC-1	**HPC-2**
Potential for cracking	ASTM C1581	Low[1]	Low[1]
1. Based on three rings having the same classification by t_{cr} > 28 days			

Recommendations for further research are:

1. Methods of sample preparation and application of cementitious coating can be investigated to realize the potential of the coating for shrinkage mitigation. This

study can consider the thickness of the coating, applying by spraying, immersing for small specimens, and scrub coating.

2. Study the chloride ion permeability and water permeability of lithium silicate-treated concrete surfaces. This is to establish a characterization method for permeability when electrical methods do not apply.
3. Study the compatibility of cementitious materials with shrinkage mitigation admixtures and the effect of dispersion methods. This will provide guidance on how to select and use shrinkage control additives for New Jersey materials.
4. Study the effect of combining shrinkage cracking mitigation methods such as the ones studied in this research.

REFERENCES

[1]   B. Wan, C. M. Foley and J. Komp, "Concrete Cracking in New Bridge Decks and Overlays, Wisconsin Highway Research Program Report, WHRP 10-05," Wisconsin Highway Research Program, 2010.

[2]   D. A. Whiting, R. J. Detwiler and E. S. Lagergren, "Cracking Tendency and Drying Shrinkage of Silica Fume Concrete for Bridge Deck Applications," *ACI Materials Journal,* vol. 97, no. 1, pp. 71-78, 2000.

[3]   S. P. Shah, W. J. Weiss and W. Yang, "Shrinkage Cracking in High Performance Concrete," in *Proceeding of PCI/FHWA International Symposium on High Performance Concrete*, New Orleans, LA, 1997.

[4]   S. M. Tarr and J. A. Farny, Concrete Floors on Ground, EB075, Fourth Edition, Skokie, Illinois, USA. : Portland Cement Association, 2008.

[5]   P. D. Krauss and E. A. Rogalla, "Transverse cracking in newly constructed bridge decks, NCHRP Rep. No. 380," Transportation Research Board, National Research Council, Washington, D.C., 1996.

[6]   S. Miyazawa and P. J. M. Monteiro, "Volume Change of High-strength Concrete in Moist Conditions," *Cement and Concrete Research,* vol. 26, no. 4, pp. 567-572, 1996.

[7]   D. Cusson and T. Hoogeveen, "An Experimental Approach for the Analysis of Early-age Behaviour of High-performance Concrete Structures under Restrained Shrinkage," *Cement and Concrete Research,* vol. 37, pp. 200-209, 2007.

[8]   Y. Yun and I. Jan, "The Experimental Research on Autogenous Shrinkage Property of HPC Column," in *Creep, Shrinkage and Durability Mechanics of Concrete and Concrete Structures: Proceedings of the CONCREEP 8*, Ise-Shima, Japan, 2008.

[9]   K. M. Lee, H. K. Lee, S. H. Lee and G. Y. Kim, "Autogenous Shrinkage of Concrete Containing Granulated Blast-furnace Slag," *Cement and Concrete*

Research, vol. 36, pp. 1279-1285, 2006.

[10] B. Persson, "Experimental Studies on Shrinkage of High-performance Concrete," *Cement and Concrete Research,* vol. 28, no. 7, pp. 1023-1036, 1998.

[11] Y. Yang, R. Sato and K. Kawai, "Autogenous shrinkage of high-strength concrete containing silica fume under drying at early ages," *Cement and Concrete Research,* vol. 35, no. 3, pp. 449-456, 2005.

[12] S. Kawashima and S. Shah, "Early-age autogenous and drying shrinkage behavior of cellulose fiber-reinforced cementitious materials," *Cement and Concrete Composites,* vol. 33, no. 2, pp. 201-208, 2011.

[13] T. Rougelot, F. Skoczylas and N. Burlion, "Water desorption and shrinkage in mortars and cement pastes: experimental study and poromechanical model," *Cement and Concrete Research,* vol. 39, pp. 36-44, 2009.

[14] S. Igarashi, A. Bentur and K. Kovler, "Autogenous Shrinkage and Induced Restraining Stresses in High-Strength Concretes," *Cement and Concrete Research,* vol. 30, no. 11, pp. 1701-1707, 2000.

[15] A. Darquennes, S. Staquet, M.-P. Delplancke-Ogletree and B. Espion, "Effect of autogenous deformation on the cracking risk of slag cement concretes," *Cement and Concrete Composites,* vol. 33, no. 3, pp. 368-379, 2011.

[16] M. Sule and K. van Breugel, "The effect of reinforcement on early-age cracking due to autogenous shrinkage and thermal effects," *Cement and Concrete Composites,* vol. 26, no. 5, pp. 581-587, 2004.

[17] S. Mindess and J. Young, Concrete, Englewood Cliffs, N.J.: Prentice-Hall, 1981.

[18] S. D. E. a. A. P. Leepage, "Control of the Development of Autogenous Shrinkage – Part I: Small Concrete Specimens," in *International Symposium on High-Performance and Reactive Powder Concretes, Ed. Aitcin, P.C. and Delagrave, Y.*, Sherbrooke, Canada, 1998, pp. 347-364.

[19] N. S. Berke, M. Dallaire, M. C. Hicks and A. Kerkar, "New Deveopments in Shrinkage-Reducing Admixtures," *ACI Symposium Publication,* vol. 173, pp. 973-1000, 1997.

[20] D. Bentz, M. Geiker and K. Hansen, "Shrinkage Reducing Admixtures and Early Age Desiccation in Cement Pastes and Mortars," *Cement and Concrete Research,* vol. 31, pp. 1075-1085, 2001.

[21] K. M. E. a. S. M. Shah S. P., "Effects of Shrinkage-Reducing Admixtures on Restrained Shrinkage Cracking of Concrete," *ACI Materials Journal,* vol. 89, no. 3, pp. 289-295, 1992.

[22] W. J. Weiss, B. B. Borischevsky and S. P. Shah., "The Influence of a Shrinkage-Reducing Admixture on the Early-Age Behavior of High-Performance Concrete," in *5th Int. Sym. on the Utilization of High-Strength/High-Performance Concrete, Vol.*

2, pp 1418-1428, Sandefjord, Norway, 1999.

[23] P. Zhan and Z. He, "Application of shrinkage reducing admixture in concrete: A review," *Construction and Building Materials,* vol. 201, pp. 676-690, 2019.

[24] K. Wang, Y. Ling, G. Lomboy and S. Sritharan, "Investigation into Shrinkage of High-Performance Concrete Used for Iowa Bridge Decks and Overlays – Phase II Shrinkage Control and Field Investigation, IHRB Project TR-690," Iowa Highway Research Board, Iowa Department of Transportation, Ames, IA, 2019.

[25] Z. Wei, G. Falzone, S. Das, N. Saklani, L. Pilon, N. Neithalath and G. Sant, "Restrained shrinkage cracking of cementitious composites containing soft PCM inclusions: A paste (matrix) controlled response," *Materials and Design,* vol. 132, pp. 367-374, 2017.

[26] Y. Peiyu and Q. Xiao, "The effect of expansive agent and possibility of delayed ettringite formation in shrinkage-compensating massive concrete," *Cement and Concrete Research,* vol. 21, no. 2, pp. 335-335, 2001.

[27] X. Yuan, W. L. Chen and H. Z.A. Lu, "Shrinkage compensation of alkali-activated slag concrete and microstructural analysis," *Construction and Building Materials,* vol. 66, pp. 422-428, 2014.

[28] L. Mo, M. Deng and W. A., "Effects of calcination condition on expansion property of MgO-type expansive agent used in cement-based materials," *Cement and Concrete Research,* vol. 40, no. 3, pp. 437-446, 2010.

[29] M. Collepardi, A. Borsoi, S. Collepardi, J. Olagot and R. Troli, "Effects of shrinkage reducing admixture in shrinkage compensating concrete under non-wet curing conditions," *Cement and Concrete Composites,* vol. 27, no. 6, pp. 704-708, 27.

[30] K. L. Y. L. G. S. S. a. S. S. Wang, "Investigation into Shrinkage of High Performance Concrete Used for Iowa Bridge Decks and Overlays – Phase II Shrinkage Control and Field Investigation, IHRB Project TR-690," Institute for Transportation, Iowa State University, Ames, IA, 2018.

[31] Z. Wei, G. Falzone, B. Wang and G. Sant, "The durability of cementitious composites containing microencapsulated phase change materials," *Cement and Concrete Composites,* vol. 81, pp. 66-76, 2017.

[32] L. Mo, M. Deng and T. M., "Effects of calcination condition on expansion property of MgO-type expansive agent used in cement-based materials," *Cement and Concrete Research,* vol. 40, no. 3, pp. 437-446, 2010.

[33] S. Monosi, R. Troli, O. Favoni and F. Tittarelli, "Effect of SRA on the expansive behaviour of mortars based on sulphoaluminate agent," *Cement and Concrete Composites,* vol. 33, pp. 485-489, 2011.

[34] R. Dong, J. Wei, Y. Qi, L. Guo, B. Chen, Y. Liu and R. Wei, "Compensation effect of expansive agent on shrinkage of self-compacting concrete," *Applied Mechanics*

and Materials, vol. 507, pp. 401-405, 2014.

[35] X. Zhu, D. Tang, Z. Zhang, Q. Li, Q. Pan and C. Yang, "Effect of Ca(OH)2 on shrinkage characteristics and microstructures of alkali-activated slag concrete.," *Construction and Building Materials,* vol. 175, pp. 467-482, 2018.

[36] H. Ye and A. Radlinska, "Shrinkage mechanisms of alkali-activated slag," *Cement and Concrete Research,* vol. 88, pp. 126-135, 2016.

[37] H. Ye and A. Radlinska, "Shrinkage mitigation strategies in alkali-activated slag," *Cement and Concrete Research,* vol. 101, pp. 131-143, 2017.

[38] Z. Jia, Y. Yang, L. Yang, Y. Zhang and Z. Sun, "Hydration products, internal relative humidity and drying shrinkage of alkali activated slag mortar with expansion agents," *Construction and Building Materials,* vol. 158, pp. 198-207, 2018.

[39] M. Haiyan, Y. Hongfa and S. Wei, "Freezing-thawing durability and its improvement high strength shrinkage compensation concrete with high volume mineral admixtures," *Construction and Building Materials,* vol. 39, pp. 124-128, 2013.

[40] S. Weber and H. Reinhardt, "A New Generation of High Performance concrete: Concrete with Autogenous Curing," *Advanced Cement Based Materials,* vol. 6, pp. 59-68, 1997.

[41] O. a. H. P. Jensen, "Water-entrained Cement Based Materials I. Principles and Theoretical Background," *Cement and Concrete Research,* vol. 31, no. 4, pp. 647-654, 2001.

[42] O. Jensen and P. Hansen, "Water-entrained Cement Based Materials II. Experimental Observations," *Cement and Concrete Research,* vol. 32, no. 6, pp. 973-978, 2002.

[43] M. Geiker, D. Bentz and O. Jensen, "Mitigating Autogenous Shrinkage by Internal Curing," in *ACI SP-218 High Performance Structural Lightweight Concrete, eds. Ries, J.P. and Holm, T.A.*, Skokie, IL, American Concrete Institute, 2004, pp. 143-154.

[44] A. Bentur, S. I. Igarashi and K. Kovler, "Prevention of autogenous shrinkage in high-strength concrete by internal curing using wet lightweight aggregates," *Cement and concrete research,* vol. 31, no. 11, pp. 1587-1591, 2001.

[45] D. P. Bentz, "Internal curing of high-performance blended cement mortars," *ACI Materials Journal,* vol. 104, no. 4, p. 408, 2007.

[46] D. Cusson and T. Hoogeveen, "Internal curing of high-performance concrete with pre-soaked fine lightweight aggregate for prevention of autogenous shrinkage cracking," *Cement and Concrete Research,* vol. 38, no. 6, pp. 757-765, 2008.

[47] P. Lura, "Internal water curing with Liapor aggregates," *Heron,* vol. 50, no. 1, pp. 5-23, 2005.

[48] A. Radlinska, F. Rajabipour, B. Bucher, R. Henkensiefken, G. Sant and J. Weiss, "Shrinkage mitigation strategies in cementitious systems: A closer look at differences in sealed and unsealed behavior," *Transportation Research Record,* vol. 2070, no. 1, pp. 59-67, 2008.

[49] S. Zhutovsky, K. Kovler and A. Bentur, "Efficiency of lightweight aggregates for internal curing of high strength concrete to eliminate autogenous shrinkage," *Materials and Structures,* vol. 35, no. 2, pp. 97-101, 2002.

[50] S. Zhutovsky, K. Kovler and A. Bentur, "Influence of cement paste matrix properties on the autogenous curing of high-performance concrete," *Cement and Concrete Composites,* vol. 26, no. 5, pp. 499-507, 2004.

[51] O. M. Jensen and P. Lura, "Techniques and materials for internal water curing of concrete," *Materials and Structures,* vol. 39, no. 9, pp. 817-825, 2006.

[52] M. Suzuki, M. S. Meddah and R. Sato, "Use of porous ceramic waste aggregates for internal curing of high-performance concrete," *Cement and Concrete Research,* vol. 39, no. 5, pp. 373-381, 2009.

[53] C. Rößler, D. D. Bui and H. M. Ludwig, "Rice husk ash as both pozzolanic admixture and internal curing agent in ultra-high performance concrete," *Cement and Concrete Composites,* vol. 53, pp. 270-278, 2014.

[54] H. K. Kim, J. G. Jang, Y. C. Choi and H. K. Lee, "Improved chloride resistance of high-strength concrete amended with coal bottom ash for internal curing," *Construction and Building Materials,* vol. 71, pp. 334-343, 2014.

[55] S. T. Yildirim, C. Meyer and S. Herfellner, "Effects of internal curing on the strength, drying shrinkage and freeze–thaw resistance of concrete containing recycled concrete aggregates," *Construction and Building Materials,* vol. 91, pp. 288-296, 2015.

[56] B. J. P. L. N. H. &. K. K. E. Mohr, "Examination of wood-derived powders and fibers for internal curing of cement-based materials," in *4th Interntational Seminar: Self-Desiccation and Its Importance in Concrete Technology (pp. 229-244)*, 2005.

[57] D. P. Bentz, P. Lura and J. W. Roberts, "Mixture proportioning for internal curing," *Concrete international,* vol. 27, no. 2, pp. 35-40, 2005.

[58] S. Ghourchian, M. Wyrzykowski, P. Lura, M. Shekarchi and B. Ahmadi, "An investigation on the use of zeolite aggregates for internal curing of concrete," *Construction and Building Materials,* vol. 40, pp. 135-144, 2013.

[59] M. Golias, J. Castro and J. Weiss, "The influence of the initial moisture content of lightweight aggregate on internal curing," *Construction and Building Materials,* vol. 35, pp. 52-62, 2012.

[60] G. Espinoza-Hijazin and M. Lopez, "Extending internal curing to concrete mixtures with W/C higher than 0.42," *Construction and Building Materials,* vol. 25, no. 3, pp. 1236-1242, 2011.

[61] V. H. Villarreal and D. A. Crocker, "Better pavements through internal hydration," *Concrete international,* vol. 29, no. 2, pp. 32-36, 2007.

[62] I. Del De la Varga, J. Castro, D. Bentz and J. Weiss, "Application of internal curing for mixtures containing high volumes of fly ash," *Cement and Concrete Composites,* vol. 34, no. 9, pp. 1001-1008, 2012.

[63] D. Cusson, Z. Lounis and L. Daigle, "Benefits of internal curing on service life and life-cycle cost of high-performance concrete bridge decks–A case study," *Cement and Concrete Composites,* vol. 32, no. 5, pp. 339-350, 2010.

[64] B. G. M. &. D. S. G. Craeye, "Super absorbing polymers as an internal curing agent for mitigation of early-age cracking of high-performance concrete bridge decks," *Construction and building materials,* vol. 25, no. 1, pp. 1-13, 2011.

[65] J. Justs, M. Wyrzykowski, D. Bajare and P. Lura, "Internal curing by superabsorbent polymers in ultra-high performance concrete," *Cement and Concrete Research,* vol. 76, pp. 82-90, 2015.

[66] D. P. Bentz and K. A. Snyder, "Protected paste volume in concrete: Extension to internal curing using saturated lightweight fine aggregate," *Cement and concrete research,* vol. 29, no. 11, pp. 1863-1867, 1999.

[67] V. Mechtcherine, M. Gorges, C. Schroefl, A. Assmann, W. Brameshuber, A. B. Ribeiro, D. Cusson, J. Custódio, E. F. d. Silva, K. Ichimiya, S.-i. Igarashi, A. Klemm and e. a. , "Effect of internal curing by using superabsorbent polymers (SAP) on autogenous shrinkage and other properties of a high-performance fine-grained concrete: results of a RILEM round-robin test," *Materials and Structures,* vol. 47, no. 3, pp. 541-562, 2014.

[68] M. J. Krafcik and K. A. Erk, "Characterization of superabsorbent poly (sodium-acrylate acrylamide) hydrogels and influence of chemical structure on internally cured mortar," *Materials and Structures,* vol. 49, no. 11, pp. 4765-4778, 2016.

[69] L. Baltazar, J. Santana, B. Lopes, M. P. Rodrigues and J. Correia, "Surface skin protection of concrete with silicate-based impregnations: influence of the substrate roughness and moisture," *Construction and Building Materials,* vol. 70, pp. 191-200, 2014.

[70] N. Z. Muhammad, A. Keyvanfar, M. Z. A. Majid, A. Sharaghat and J. Mirza, "Waterproof performance of concrete: a critical review on implemented approaches," *Construction and Building Materials,* vol. 101, pp. 80-90, 2015.

[71] X. Pan, Z. Shi, C. Shi, T. Ling and N. Li, "A review on surface treatment for concrete - part 2: performance," *Construction and Building Materials,* vol. 133, pp.

81-90, 2017.

[72] H. Y. Moon, D. G. Shin and D. S. Choi, "Evaluation of the durability of mortar and concrete applied with inorganic coating material and surface treatment system," *Construction and Building Materials,* vol. 21, pp. 362-369, 2007.

[73] S. K. Y. Y. L. B. J. a. K. S. Park, "Evaluation of concrete durability performance with sodium silicate impregnants," *Advances in Materials Science and Engineering,* vol. 1, pp. 1-11, 2014.

[74] L. S. J. L. B. R. M. P. a. C. J. Baltazar, "Surface skin protection of concrete with silicate-based impregnations: influence of the substrate roughness and moisture," *Construction and Building Materials,* vol. 70, pp. 191-200, 2014.

[75] M. Grzybowski and S. P. Shah, "Shrinkage cracking of fiber reinforced concrete," *ACI Materials Journal,* vol. 87, no. 2, pp. 138-148, 1990.

[76] B. Chen and C. Fang, "Contribution of fibres to the properties of EPS lightweight concrete," *Magazine of Concrete Research,* vol. 61, no. 9, pp. 671-678, 2009.

[77] V. C. Li and S. Wang, "Microstructure variability and macroscopic composite properties of high performance fiber reinforced cementitious composites," *Probabilistic Engineering Mechanics,* vol. 21, no. 3, pp. 201-206, 2006.

[78] A. Noushini, B. Samali and K. Vessalas, "Effect of polyvinyl alcohol (PVA) fibre on dynamic and material properties of fibre reinforced concrete," *Construction and Building Materials,* vol. 49, pp. 374-383, 2013.

[79] R. F. Zollo, "Fiber-reinforced concrete: an overview after 30 years of development," *Cement and Concrete Composites,* vol. 19, no. 2, pp. 107-122, 1997.

[80] S. Daneti, T. Wee and T. Thangayah, "Effect of polypropylene fibres on the shrinkage cracking behaviour of lightweight concrete," *Magazine of Concrete Research,* vol. 63, no. 11, pp. 871-881, 2011.

[81] D. Y. Yoo, H. O. Shin, J. M. Yang and Y. S. Yoon, "Material and bond properties of ultra high performance fiber reinforced concrete with micro steel fibers," *Composites Part B: Engineering,* vol. 58, pp. 122-133, 2014.

[82] S. Altoubat, K. A. Rieder and M. T. Junaid, "Short-and long-term restrained shrinkage cracking of fiber reinforced concrete composite metal decks: an experimental study," *Materials and Structures,* vol. 50, no. 2, p. 140, 2017.

[83] J. Susetyo, "Fibre Reinforcement for Shrinkage Crack Control in Prestressed, Precast Segmental Bridges, doctoral thesis," Department of Civil Engineering, University of Toronto, ON, Canada, 2009.

[84] P. H. Bischoff, "Tension Stiffening and Cracking of Steel FiberReinforced Concrete," *Journal of Materials in Civil Engineering,* vol. 15, no. 2, pp. 174-182,

2003.

[85] D. Saje, B. Bandelj, J. Šušteršič, J. Lopatič and F. & Saje, "Shrinkage of polypropylene fiber-reinforced high-performance concrete," *Journal of materials in civil engineering,* vol. 23, no. 7, pp. 941-952, 2010.

[86] A. Saradar, B. Tahmouresi, E. Mohseni and A. Shadmani, "Restrained shrinkage cracking of fiber-reinforced high-strength concrete," *Fibers,* vol. 6, no. 12, pp. 1-13, 2018.

[87] P. Song, S. Hwang and B. Sheu, "Strength properties of nylon and polypropylene fiber reinforced concretes," *Cement and Concrete Research,* vol. 35, pp. 1546-1550, 2005.

[88] D. Shen, J. Kang, X. Yi, L. Zhou and X. Shi, "Effect of double hooked-end steel fiber on early-age cracking potential of high strength concrete in restrained ring specimens," *Construction and Building Materials,* vol. 223, pp. 1095-1105, 2019.

[89] K. Younis, F. Ahmed and K. Najim, "Effect of recycled-steel fibers on compressive strength and shrinkage behavior of self-compacting concrete," in *11th International Conference on Developments in eSystems Engineering, pages 268 - 272*, 2018.

[90] S. Kawashima and S. Shah, "Early-age autogenous and drying shrinkage behavior of cellulose fiber-reinforced cementitious materials," *Cement and Concrete Composites,* vol. 33, no. 2, pp. 201-208, 2011.

[91] S. M. Cramer and A. J. Carpenter, "Influence of total aggregate gradation on freeze-thaw durability and other performance measures of paving concrete," *Transportation Research Record,* vol. 1668, no. 1, pp. 1-8, 1999.

[92] J. Shilstone, "Concrete mixture optimization," *Concrete International,* vol. 12, no. 6, pp. 33-39, 1990.

[93] V. Ramakrishnan and A. Patnaik, "Implementation of high performance concrete with optimized aggregate gradation and flyash in bridge decks," in *Proceedings of the First International Conference on Recent Advances in Concrete Technology*, Washington, D.C., 2007.

[94] D. W. Fowler and M. M. Rached, "Optimizing aggregates to reduce cement in concrete without reducing quality," *Transportation Research Record,* vol. 2240, pp. 89-95, 2011.

[95] R. D. Hooten, M. Anson-Cartwright and U. Schutz, "Improved durability and sustainability of concretes using combined aggregate gradation," in *Concrete Structures for Sustainable Community, Edited by Dirch H. Bager and Johan Silfwerbrand, Royal Institute of Technology*, Stockholm, Sweden, 2012.

[96] J. a. L. D. Henschen, "Performance of concrete with high aggregate packing density," *Journal of the Chinese Ceramic Society,* vol. 40, no. 1, pp. 27-32, 2012.

[97] S. W. Ryu and H. Kim, "Development of lower shrinkage and reflection material for concrete pavement," *International Journal of Pavement Engineering,* vol. 17, no. 8, pp. 709-715, 2016.

[98] W. Zhu, J. Wei, F. Li, T. Zhang, Y. Chen, J. Hu and Q. Yu, "Understanding the restraint effect of coarse aggregate on the drying shrinkage of self-compacting concrete," *Construction and Building Materials,* vol. 114, pp. 458-463, 2016.

[99] M. S. Meddah, M. Suzuki and R. Sato, "Influence of a combination of expansive and shrinkage-reducing admixture on autogenous deformation and self-stress of silica fume high-performance concrete," *Construction and Building Materials,* vol. 25, pp. 239-250, 2011.

[100] M. J. Oliveira, A. B. Ribeiro and F. G. Branco, "Combined effect of expansive and shrinkage reducing admixtures to control autogenous shrinkage in self-compacting concrete," *Construction and Building Materials,* vol. 52, pp. 267-275, 2014.

[101] R. Khajehdehi, M. Feng, D. Darwin, J. Lafikes, E. K. Ibrahim and M. O'Reilly, "Combined effects of internal curing, SCMs, and expansive additives on concrete shrinkage," *Advances in Civil Engineering Materials,* vol. 7, no. 4, pp. 644-659, 2018.

[102] M. Valipour and K. Khayat, "Coupled effect of shrinkage-mitigating admixtures and saturated lightweight sand on shrinkage of UHPC for overlay applications," *Construction and Building Materials,* vol. 184, pp. 320-329, 2018.

[103] H. Nassif, K. Aktas, H. Najm and N. Suksawang, "Concrete Shrinkage Analysis of Bridge Deck Concrete, Report No. FHWA NJ-2007-007," Dept. of Civil & Environmental Engineering, Center for Advanced Infrastructure & Transportation, Piscataway, NJ, 2007.

[104] C. Ramseyer and J. Giebler, "Use of high performance concrete in Oklahoma bridge decks. FHWA-OK-10-03," Oklahoma Department of Transportation Planning and Research Division, Oklahoma City, OK, 2010.

[105] S. A. a. C. R. W. Durham, "Evaluation of CDOT specifications for class H and Class HT crack resistant concretes. Report No. CDOT-2010-5," Colorado Department of Transportation - Research , Denver, CO, 2010.

[106] K. Wang, S. Schlorholtz, S. Sritharan, H. Seneviratne, X. Wang and Q. Hou, "Investigation into Shrinkage of High-Performance Concrete Used for Iowa Bridge Decks and Overlays, Report No. IHRB Project TR-633," Institute for Transportation, Iowa State University, Ames, IA, 2013.

[107] R. L. Varner, "Shrinkage and durability study of bridge deck concrete, FHWA/MS-DOT-RD-09-216," Mississippi Department of Transportation, Jackson, MS , 2010.

[108] South Dakota Department of Transportation, Standard Specifications for Roads and Bridges, Pierre, SD: South Dakota Department of Transportation, 2015.

[109] Colorado Department of Transportation, Standard Specifications for Road and Bridge Construction, Denver, CO: Colorado Department of Transportation, 2017.

[110] A. Pott and J. Elkaissi, "High Performance Concrete in Colorado," 1 5 2009. [Online]. Available: http://concretebridgeviews.com/2009/05/high-performance-concrete-in-colorado/. [Accessed 15 November 2022].

[111] Colorado Department of Transportation, Standard Specifications for Road and Bridge Construction, Denver, CO: Colorado Department of Transportation, 2022.

[112] Kansas Department of Transportation, Standard Specifications For State Road & Bridge Construction, Topeka, KS: Kansas Department of Transportation, 2015.

[113] Delaware Department of Transportation, Standard Specifications for Road and Bridge Construction, Dover, DE: Delaware Department of Transportation, 2022.

[114] New Jersey Department of Transportation, Standard Specifications for Road and Bridge Construction, Ewing Township, New Jersey: New Jersey Department of Transportation, 2019.

[115] D. Bentz and J. Weiss, "nternal Curing: A 2010 State-of-the-Art Review, NIST Interagency/Internal Report (NISTIR)," National Institute of Standards and Technology, Gaithersburg, MD, 2011.

[116] ASTM C157, "Standard Test Method for Length Change of Hardened Cement Mortar and Concrete," in *ASTM Annual Book of Standards*, West Conshohocken, PA, ASTM International, 2014, p. 7.

[117] ASTM C1581, "Standard Test Method for Determining Age at Cracking and Induced Tensile Stress Characteristics of Mortar and Concrete under Restrained Shrinkage," in *ASTM Annual Book of Standards*, West Conshohocken, PA, ASTM International, 2022, p. 7.

[118] ASTM C39, "Standard Test Method for Compressive Strength of Cylindrical Concrete Specimens," in *ASTM Annual Book of Standards*, West Conshohocken, PA, ASTM International, 2022, p. 8.

[119] ASTM C496, "Standard Test Method for Splitting Tensile Strength of Cylindrical Concrete Specimens," in *ASTM Annual Book of Standards*, West Conshohocken, PA, ASTM International, 2022, p. 4.

[120] ASTM C469, "Standard Test Method for Static Modulus of Elasticity and Poisson's Ratio of Concrete in Compression," in *ASTM Annual Book of Standards*, West Conshohocken, PA, ASTM International, 2022, p. 5.

[121] ASTM C512, "Standard Test Method for Creep of Concrete in Compression," in *ASTM Annual Book of Standards*, West Conshohocken, PA, ASTM International, 2022, p. 5.

[122] AASHTO T358, "Standard Method of Test for Surface Resistivity Indication of Concrete's Ability to Resist Chloride Ion Penetration," Washington, D.C., American

Association of State Highway and Transportation Officials, 2021, p. 10.

[123] ASTM C666, "Standard Test Method for Resistance of Concrete to Rapid Freezing and Thawing," in *ASTM Annual Book of Standards*, West Conshohocken, PA, ASTM International, 2022, p. 6.

[124] R. Spragg, Y. Bu, K. Snyder, D. Bentz and J. Weiss, "Electrical Testing of Cement-Based Materials: Role of Testing Techniques, Sample Conditioning, and Accelerated Curing - FHWA/IN/JTRP-2013/28," Indiana Department of Transportation and Purdue University, West Lafayette, Indiana, 2013.